Nonperturbative renormalization group and momentum dependence of *n*-point functions. I

Jean-Paul Blaizot*
ECT, Villa Tambosi, strada delle Tabarelle 286, 38050 Villazzano (TN), Italy*

Ramón Méndez-Galain† and Nicolás Wschebor‡
Instituto de Física, Facultad de Ingeniería, J.H.y Reissig 565, 11000 Montevideo, Uruguay
(Received 31 March 2006; published 21 November 2006)

We present an approximation scheme to solve the nonperturbative renormalization group equations and obtain the full momentum dependence of the *n*-point functions. It is based on an iterative procedure where, in a first step, an initial ansatz for the *n*-point functions is constructed by solving approximate flow equations derived from well motivated approximations. These approximations exploit the derivative expansion and the decoupling of high momentum modes. The method is applied to the O(*N*) model. In leading order, the self-energy is already accurate both in the perturbative and the scaling regimes. A stringent test is provided by the calculation of the shift ΔT_c in the transition temperature of the weakly repulsive Bose gas, a quantity which is particularly sensitive to all momentum scales. The leading order result is in agreement with lattice calculations, albeit with a theoretical uncertainty of about 25%.

DOI: 10.1103/PhysRevE.74.051116 PACS number(s): 05.10.Cc, 03.75.Nt, 11.10.Wx

I. INTRODUCTION

The need for reliable and efficient nonperturbative calculation methods is felt, in various forms, in nearly all fields of physics: in nuclear and particle physics (to deal with the infrared sector of quantum chromodynamics and the associated phenomena of color confinement and chiral symmetry breaking), in condensed matter and statistical physics of systems in or out of equilibrium (phase transitions and critical phenomena, disorder systems, strongly correlated electrons), to quote but just a few general examples. In many of these cases, the absence of a small parameter prevents one to build a solution in terms of a systematic expansion. In order to treat such problems, what one needs is a nonperturbative method that allows the calculation of correlation functions for arbitrary values of the external momenta, from which most physical quantities can be deduced.

Among the nonperturbative methods that have been developed along the years, the nonperturbative renormalization group (NPRG) [1–5] stands out as a very promising tool, suggesting new approximation schemes which are not easily formulated in other, more conventional, approaches in field theory or many body physics. The NPRG has been applied successfully to a variety of physical problems, in condensed matter, particle or nuclear physics (for reviews, see, e.g., Refs. [6–8]). In most of these problems, however, the focus is on long wavelength modes and the solution of the NPRG equations involves generally a derivative expansion which only allows for the determination of the *n*-point functions and their derivatives at small external momenta (vanishing momenta in the case of critical phenomena). In many situations, this is not enough: a full knowledge of the momentum dependence of the correlation functions is needed to calculate the quantities of physical interest (e.g., to get the spectrum of excitations, the shape of the Fermi surface, the scattering matrix, etc.).

The NPRG presents itself as an infinite hierarchy of equations relating sequentially the various *n*-point functions. To our knowledge, most efforts to solve this hierachy, aside from the derivative expansion alluded to above, have been based on various forms of the early proposal by Weinberg [9], that is, they involve some truncation of the infinite tower of flow equations for the *n*-point functions, ignoring higher order vertices, or possibly using various *Ansätze* for some of them [10,11]. This leads to approximations similar to those used when solving the hierarchy of Schwinger-Dyson equations [12]. However, despite the fact that very encouraging results have been obtained this approximation scheme presents convergence difficulties [13].

The goal of this paper is then to present a method for solving the NPRG equations that keeps the contribution of all the vertices present in the flow equations. This is achieved by exploiting specific properties of the NPRG. The method allows one to get, in a relatively simple way, the full momentum dependence of the *n*-point functions. It involves iterations that start with an initial guess for the *n*-point functions. That initial guess is then injected in the flow equations which are integrated in order to obtain a leading order expression for the *n*-point functions. And so on. Clearly, each new iteration involves more *n*-point functions, and the scheme may become rapidly prohibitively complicated. It is therefore crucial that the starting point of the iterations, that is, the initial *Ansatz* for the *n*-point functions, be as close as possible to the exact solution, in order to get a good approximation with a minimum number of iterations. The construction of this initial *Ansatz* is therefore the central part of the method.

To derive this initial *Ansatz* we shall first simplify the flow equations using well motivated approximations. We shall exploit a modified derivative expansion in its leading order and the decoupling of high momentum modes in the flow equations in order to simplify the momentum depen-

*Electronic address: blaizot@ect.it
†Electronic address: mendezg@fing.edu.uy
‡Electronic address: nicws@fing.edu.uy

dence of the vertices that govern the flow. The resulting approximate equations are then solved explicitly.

The particular class of problems that we are concerned with can be formulated in terms of a field theory, and as a generic case, we shall consider here a scalar ϕ^4 theory in d dimension with O(N) symmetry:

$$S = \int d^d x \left\{ \frac{1}{2}[\nabla \varphi(x)]^2 + \frac{1}{2} r \varphi^2(x) + \frac{u}{4!}[\varphi^2(x)]^2 \right\}, \quad (1)$$

where the field $\varphi(x)$ has N real components $\varphi_i(x)$, with $i = 1, \ldots, N$. We emphasize, however, that most of the arguments presented in this paper have a wider range of applicability.

In this paper, we shall apply the method to the calculation of the self-energy at criticality and at zero external field, in leading order and in $d=3$. This involves getting the initial *Ansatz* for both the propagator and the four-point function. Constructing this initial *Ansatz* is the main task carried out in the present paper. It is presented in Sec. III, together with a more detailed description of the approximation scheme. First, in Sec. II, we review basic features of the NPRG, and illustrate various strategies that have been used to obtain solutions of the flow equations. These will provide the necessary background to motivate the approximation scheme presented in Sec. III, as well as the approximations involved in the construction of the initial *Ansatz* for the four-point function. The reader familiar with the NPRG may skip this section and go directly to Sec. III. The results for the self-energy are presented in Sec. IV.

The self-energy thus obtained has the correct behavior at all momenta. It agrees with perturbation theory in the ultraviolet and it presents the expected power-law behavior in the infrared. As a benchmark for our approximation scheme we shall use the shift ΔT_c of the transition temperature of a weakly interacting Bose gas [14,15] (see also Ref. [16] for a recent review on the theory of the weakly interacting Bose gas). As we shall recall later, the precise evaluation of ΔT_c requires an accurate knowledge of a two-point function at all momentum scales, and it constitutes therefore a very stringent test of any method aiming at getting the full momentum dependence of n-point functions. As shown in Ref. [14], the calculation of ΔT_c reduces to that of the change $\Delta\langle\varphi^2\rangle$ of the magnitude of the fluctuations of the field described by the action (1), for $d=3$ and $N=2$ [17]. This calculation can be done immediately once the self-energy is known. It is presented in Sec. IV B together with a comparison with estimates of this quantity using different techniques, for instance lattice calculations [18,19].

In a companion paper [20] that we shall call Paper II, we extend the method described here to the next-to-leading order calculation of the self-energy (which involves the leading order calculation of the four-point function). Some of the results of this study have already been presented in Ref. [21]. However, since the publication of Ref. [21], we have been able to improve the accuracy of the leading order calculation of the four-point function, which yields a considerable improvement of the next-to-leading order self-energy; the final results that we obtain for ΔT_c are in excellent agreement with the lattice calculations, with a much reduced theoretical uncertainty as compared with the estimates presented in the present paper (see Paper II). Further progress has been achieved in an effort to get rid of some of the approximations used in the present work, and which contributes to the theoretical uncertainty in the predictions. A possible strategy to do so has been presented in Ref. [22], and first results concerning its numerical implementation will be presented shortly [23].

II. SOME FEATURES OF THE NPRG EQUATIONS

A. Generalities

The NPRG allows the construction of a set of effective actions $\Gamma_\kappa[\phi]$ which interpolate between the classical action S and the full effective action $\Gamma[\phi]$: In $\Gamma_\kappa[\phi]$ the magnitude of long wavelength fluctuations of the field is controlled by an infrared regulator depending on a continuous parameter κ which has the dimension of a momentum. The full effective action is obtained for the value $\kappa=0$, the situation with no infrared cutoff and where therefore all fluctuations are taken into account. In the other limit, corresponding to a value of κ of the order of a microscopic scale Λ at which fluctuations are suppressed, $\Gamma_{\kappa=\Lambda}[\phi]$ reduces to the classical action [44].

In practice the control of the magnitude of the fluctuations is implemented by adding to the classical action (1) the regulator

$$\Delta S_\kappa[\varphi] = \frac{1}{2} \int \frac{d^d q}{(2\pi)^d} \varphi_i(q) R_\kappa(q) \varphi_i(-q), \quad (2)$$

where R_κ denotes a family of "cutoff functions" depending on κ. The role of ΔS_κ is to suppress the fluctuations with momenta $q \lesssim \kappa$, while leaving unaffected those with $q \gtrsim \kappa$. Thus, typically, $R_\kappa(q) \to \kappa^2$ when $q \ll \kappa$, and $R_\kappa(q) \to 0$ when $q \gtrsim \kappa$. There is a large freedom in the choice of $R_\kappa(q)$, abundantly discussed in the literature [24–27]. The choice of the cutoff function matters when approximations are done, as is the case in all situations of practical interest. We have used in this work the cutoff function proposed in Ref. [24]:

$$R_\kappa(q^2) \propto (\kappa^2 - q^2)\theta(\kappa^2 - q^2). \quad (3)$$

This regulator allows many calculations to be done analytically. It is known to work well with the derivative expansion in leading order, which we shall use in this work.

For each value of κ, one defines the generating functional of connected Green's functions,

$$W_\kappa[J] = \ln \int D\varphi \exp\left\{ -S[\varphi] - \Delta S_\kappa[\varphi] + \int d^d x \varphi(x) J(x) \right\}. \quad (4)$$

We have, for instance,

$$\phi_{\kappa,J}(x) \equiv \langle \varphi(x) \rangle_{\kappa,J} = \frac{\delta W_\kappa}{\delta J(x)}. \quad (5)$$

The Feynman diagrams contributing to W_κ are those of ordinary perturbation theory, except that the propagators contain

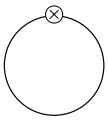

FIG. 1. Diagrammatic illustration of the right-hand side of the flow equation of the effective action, Eq. (7). The crossed circle represents an insertion of $\partial_\kappa R_\kappa$, and the thick line is a full propagator in an arbitrary background field.

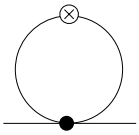

FIG. 2. Diagrammatic illustration of the rhs of the flow equation for the two-point function, Eq. (9). The black dot denotes the four-point function and the thick line is the full propagator G. The circled cross represents the insertion of $\partial_\kappa R_\kappa$.

the infrared regulator. We also define the effective action, through a modified Legendre transform that includes the explicit subtraction of ΔS_κ:

$$\Gamma_\kappa[\phi] = -W_\kappa[J_\phi] + \int d^d x \phi(x) J_\phi(x) - \Delta S_\kappa[\phi], \qquad (6)$$

where J_ϕ is obtained by inverting Eq. (5). Note that, in this inversion, ϕ is considered as a given variable, so that J_ϕ becomes implicitly dependent on κ.

One can write an exact flow equation for $\Gamma_\kappa[\phi]$ which gives its variation as a function of κ, at fixed ϕ. It reads [1–5]

$$\partial_\kappa \Gamma_\kappa[\phi] = \frac{1}{2}\,\mathrm{tr} \int \frac{d^d q}{(2\pi)^d} \partial_\kappa R_\kappa(q^2)[\Gamma_\kappa^{(2)} + R_\kappa]^{-1}_{q,-q}, \qquad (7)$$

where $\Gamma_\kappa^{(2)}$ is the second derivative of Γ_κ with respect to ϕ, and the trace tr runs over the O(N) indices. Equation (7) is the master equation of the NPRG. Its right-hand side has the structure of a one loop integral, with one insertion of $\partial_\kappa R_\kappa(q^2)$ (see Fig. 1). The solution of Eq. (7) yields the effective action $\Gamma[\phi]=\Gamma_{\kappa=0}[\phi]$ starting with the initial condition $\Gamma_{\kappa=\Lambda}[\phi]=S[\phi]$ (see, e.g., Ref. [6]).

As is well known (see, e.g., Ref. [28]), the effective action $\Gamma[\phi]$ is the generating functional of the one-particle irreducible n-point functions. This property extends trivially to $\Gamma_\kappa[\phi]$. Since we shall be concerned only with n-point functions for constant (eventually vanishing) external fields we exploit translational invariance to define reduced n-point functions $\Gamma^{(n)}(\kappa;p_1,\ldots,p_n)$ as follows:

$$(2\pi)^d \delta^{(d)}(p_1 + \cdots + p_n)\Gamma^{(n)}(\kappa;p_1,\ldots,p_n) = \int d^d x_1 \cdots \int d^d x_n e^{i\Sigma_{j=1}^n p_j \cdot x_j} \left.\frac{\delta^n \Gamma_\kappa[\phi]}{\delta\phi(x_1)\cdots\delta\phi(x_n)}\right|_{\phi=\mathrm{cst}}. \qquad (8)$$

By differentiating Eq. (7) with respect to ϕ, and then letting the field be zero, one gets the flow equations for all n-point functions in a vanishing background field ϕ. For example, the equation for the two-point function reads

$$\partial_\kappa \Gamma_{12}^{(2)}(\kappa;p) \equiv \delta_{12}\partial_\kappa \Sigma(\kappa;p) = -\frac{1}{2}\int \frac{d^d q}{(2\pi)^d} \partial_\kappa R_\kappa(q) G^2(\kappa;q) \times \Gamma^{(4)}_{12ll}(\kappa;p,-p,q,-q), \qquad (9)$$

where we have introduced the self-energy $\Sigma(\kappa;q)$ and

$$G^{-1}(\kappa,q) = q^2 + R_\kappa(q) + \Sigma(\kappa;q). \qquad (10)$$

In Eq. (9), and later in this paper, we often denote simply by numbers 1, 2, etc., the O(N) indices i_1, i_2, etc., in order to alleviate the notation. A diagrammatic illustration of the right-hand side of Eq. (9) is given in Fig. 2. Similarly, the flow of the four-point function in vanishing field reads

$$\begin{aligned}\partial_\kappa \Gamma^{(4)}_{1234}(\kappa;p_1,p_2,p_3,p_4) = \int \frac{d^d q}{(2\pi)^d} \partial_\kappa R_k(q^2) G^2(\kappa;q) \{ & G(\kappa;q+p_1+p_2)\Gamma^{(4)}_{12ij}(\kappa;p_1,p_2,q,-q-p_1-p_2) \\ & \times \Gamma^{(4)}_{34ij}(\kappa;p_3,p_4,-q,q-p_3-p_4) + G(\kappa;q+p_1+p_3)\Gamma^{(4)}_{13ij}(\kappa;p_1,p_3,q,-q-p_1-p_3) \\ & \times \Gamma^{(4)}_{24ij}(\kappa;p_2,p_4,-q,q-p_2-p_4) + G(\kappa;q+p_1+p_4)\Gamma^{(4)}_{14ij}(\kappa;p_1,p_4,q,-q-p_1-p_4) \\ & \times \Gamma^{(4)}_{32ij}(\kappa;p_3,p_2,-q,q-p_3-p_2)\} - \frac{1}{2}\int \frac{d^d q}{(2\pi)^d} \partial_\kappa R_\kappa(q) G^2(\kappa;q) \Gamma^{(6)}_{1234ii}(\kappa;p_1,p_2,p_3,p_4,q,-q).\end{aligned} \qquad (11)$$

The four contributions in the rhs. of Eq. (11) are represented in the diagrams shown in Figs. 3 and 4.

Equations (9) and (11) for the two- and four-point functions constitute the beginning of an infinite hierarchy of exact equations for the n-point functions, with the flow equation for the n-point function involving all the m-point functions up to $m=n+2$. Clearly, solving this hierarchy requires approximations. In the rest of this section we discuss

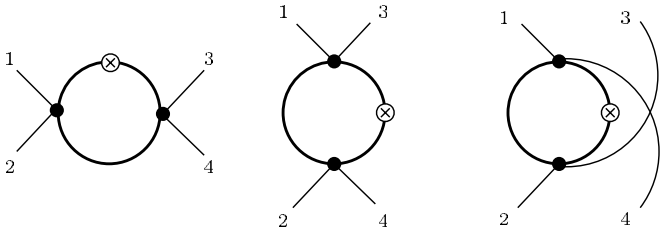

FIG. 3. Diagrammatic illustration of the rhs of the flow equation for the four-point function, Eq. (11): contribution of the four-point functions (represented by black disks) in the three channels s, t, and u, from left to right. The crossed circle represents an insertion of $\partial_\kappa R_\kappa$, and the thick line is a full propagator.

various approximations that are commonly used in the context of the NPRG, and that we shall exploit in the more general scheme presented in the next section. In the next subsection we recall how perturbation theory can be recovered from the hierarchy through an iterative procedure. Then, we focus on the regime of small momenta where an expansion in powers of gradients of the field often yield accurate results. In particular we briefly discuss the leading order of this expansion, the local potential approximation (LPA). Finally, in the last subsection, we review simple properties of correlation functions of the O(N) model in the limit of large N: this will provide a simple, yet nontrivial, example in which the momentum dependence of correlation functions can be analyzed in detail.

B. Perturbation theory

Perturbation theory can be recovered by solving the exact flow equations iteratively, starting with the classical action as initial input (see, e.g., Refs. [29,30]). The perturbative expansion of the effective action, or equivalently the loop expansion, is controlled by a "small parameter," namely $\hbar$. Making this parameter explicit one rewrites Eq. (7) as

$$\partial_\kappa \Gamma_\kappa[\phi] = \frac{\hbar}{2} \mathrm{Tr}\, \partial_\kappa R_\kappa [\Gamma_\kappa^{(2)} + R_\kappa]^{-1}, \tag{12}$$

and then proceed to the expansion in powers of $\hbar$. In leading order $\Gamma_\kappa[\phi]$ is independent of κ and is equal to the classical action:

$$\Gamma_\kappa^{[0]}[\phi] = S[\phi] + \mathcal{O}(\hbar). \tag{13}$$

The solution of this equation can be used to obtain an approximation for the two-point function $\Gamma_\kappa^{(2)}[\phi]$, by taking the second derivative of $S[\phi]$ with respect to ϕ [see Eq. (8)]. At the next iteration this is used in the right-hand side of Eq. (12) in order to obtain the order 1 correction to $\Gamma_\kappa[\phi]$. One gets then, after integrating the flow equation from Λ to κ (using the fact that $S^{(2)}$ is independent of κ),

$$\Gamma_\kappa^{[1]}[\phi] = S[\phi] + \frac{\hbar}{2} \mathrm{Tr} \ln \left[\frac{S^{(2)} + R_\kappa}{S^{(2)} + R_\Lambda} \right] + \mathcal{O}(\hbar^2), \tag{14}$$

where one recognizes the familiar one-loop expression of the effective action. One can repeat the procedure and show that, after n iterations, one reproduces the result that one would obtain by calculating $\Gamma_\kappa[\phi]$ using perturbation theory at order n loop (with the infrared cutoff).

In the case of massless theories, which we are interested in here, this iteration scheme is applicable only for values of κ not too small. Indeed, in general, perturbation theory stops to make sense [28] when $\kappa \lesssim \kappa_c$, with $\kappa_c \sim u^{1/(4-d)}$, where u is the coupling constant defined in Eq. (1) (concrete estimates of κ_c will be presented in the next subsection). When $\kappa \to 0$, perturbative calculations may lead to infrared divergent expressions. This difficulty is particularly important in the scaling regime, where $p \ll p_c \sim \kappa_c$. Other approximation schemes are then required.

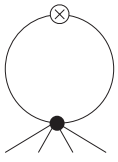

FIG. 4. Diagrammatic illustration of the rhs of the flow equation for the four-point function, Eq. (11): contribution of the six-point function $\Gamma^{(6)}$ (represented by a black disk). The crossed circle represents an insertion of $\partial_\kappa R_\kappa$, and the thick line is a full propagator.

C. Local potential approximation

The derivative expansion offers the possibility to calculate some properties of the scaling regime. It exploits the fact that the shape of the regulator in the flow equations [e.g., Eqs. (9) or (11)] forces the loop momentum q to be smaller than κ, i.e., only momenta $q \lesssim \kappa$ contribute to the flow. Besides, in general, the regulator insures that, as long as $\kappa \neq 0$, all vertices are smooth functions of momenta [45]. Then, in the calculation of the n-point functions at small external momenta p_i, it is possible to expand the n-point functions in the rhs of the flow equations in terms of q^2/κ^2 and p_i^2/κ^2, or equivalently in terms of the derivatives of the field. Note, however, that since eventually $\kappa \to 0$, such an expansion strictly makes sense only for $p_i = 0$, unless there is a mass in the problem.

In leading order, this procedure reduces to the so-called local potential approximation (LPA), which assumes that the effective action has the form

$$\Gamma_\kappa^{LPA}[\phi] = \int d^d x \left\{ \frac{1}{2} \partial_\mu \phi_i \partial_\mu \phi_i + V_\kappa(\rho) \right\}, \tag{15}$$

where $\rho \equiv \phi_i \phi_i / 2$. The derivative term here is simply the one appearing in the classical action, and $V_\kappa(\rho)$ is the effective potential. The exact flow equation for V_κ is easily obtained by assuming that the field ϕ is constant in Eq. (7). One needs, however, to take into account the O(N) symmetry, and to decompose the propagator of the scalar field in a constant background ϕ_i into its transverse (G_T) and longitudinal (G_L) components:

$$G_{ij}(\kappa;q) = G_T(\kappa;q) \left(\delta_{ij} - \frac{\phi_i \phi_j}{2\rho} \right) + G_L(\kappa;q) \frac{\phi_i \phi_j}{2\rho}. \tag{16}$$

Then the equation for the potential reads

$$\partial_\kappa V_\kappa(\rho) = \frac{1}{2}\int \frac{d^d q}{(2\pi)^d}\partial_\kappa R_\kappa(q)\{(N-1)G_T(\kappa;q) + G_L(\kappa;q)\}. \tag{17}$$

By using the LPA effective action, Eq. (15), one gets

$$G_T(\kappa;q) = \frac{1}{q^2 + V'(\rho) + R_k(q)},$$

$$G_L(\kappa;q) = \frac{1}{q^2 + V'(\rho) + 2\rho V''(\rho) + R_\kappa(q)}, \tag{18}$$

with $V'(\rho)=dV/d\rho$ and $V''(\rho)=d^2V/d\rho^2$. With these propagators, Eq. (17) becomes then a closed equation.

Higher order corrections to the LPA include terms in the effective action with an increasing number of derivatives. Although there is no formal proof of convergence, the derivative expansion exhibits quick apparent convergence if the regulator $R_\kappa(q)$ is appropriately chosen [24,27,31]. In practice, the LPA reproduces well the physical quantities dominated by small momenta (such as the effective potential or critical exponents) in all theories where it has been tested (see, for example, Refs. [6,8]). Higher order corrections lead to significant improvements [32], and the derivative expansion has been pushed up to third order [31], yielding critical exponents in the Ising universality class of the same level of precision as those obtained with the best accepted methods (see, e.g., Ref. [31]).

An interesting improvement of the LPA, which we refer to as the LPA′, takes into account a running field renormalization constant Z_κ and allows for a nontrivial anomalous dimension, determined from the cutoff dependence of Z_κ [1]. In the LPA′, the effective action is assumed to be of the form

$$\Gamma_\kappa^{LPA'}[\phi] = \int d^d x\left\{\frac{Z_\kappa}{2}\partial_\mu\phi_i\partial_\mu\phi_i + V_\kappa(\rho)\right\}, \tag{19}$$

where Z_κ is a function of κ (and not of ρ). It is useful to explicitly include the field normalization in the regulator (3), i.e., we redefine R_κ by multiplying it by the factor Z_κ. Thus the regulator used in the present work becomes

$$R_\kappa(q) = Z_\kappa(\kappa^2 - q^2)\Theta(\kappa^2 - q^2). \tag{20}$$

The factor Z_κ is determined from the flow equation for $\Gamma_\kappa^{(2)}$ in a constant external field, which can be derived from Eq. (7). The vertices and propagators entering this equation are those dictated by the form (19) assumed for the effective action. By expanding the resulting equation to order p^2: $\Gamma^{(2)}(\kappa;p) - \Gamma^{(2)}(\kappa;0) \sim p^2 Z_\kappa$ [recall that for nonvanishing κ, $\Gamma^{(2)}(\kappa;p)$ is a smooth function of p], one obtains the following equation for Z_κ [6]:

$$\partial_\kappa Z_\kappa = \frac{4}{d}\rho_0(V''(\rho_0))^2\,\tilde{\partial}_\kappa \int \frac{d^d q}{(2\pi)^d} q^2 G_L^2(\kappa;q)G_T^2(\kappa;q) \times[Z_\kappa + R_\kappa'(q)]^2, \tag{21}$$

where $R_\kappa'(q) \equiv \partial R_\kappa(q)/\partial q^2$, the derivative $\tilde{\partial}_\kappa$ acts only on the explicit factors R_κ (and their derivatives), and ρ is fixed at its running minimum $\rho=\rho_0$ (which depends on κ). The anomalous dimension is related to Z_κ by (see, e.g., Ref. [6]; for a simple proof, see Appendix A):

$$\eta_\kappa = -\kappa\partial_\kappa \ln Z_\kappa. \tag{22}$$

In the LPA′ the flow equation for the effective potential is the same as in the LPA, Eq. (17), except for the replacement $q^2 \to Z_\kappa q^2$ in the propagators. It follows that the flow equation for the potential is coupled with the flow equation for Z_κ, Eq. (21).

The derivatives of $V_\kappa(\rho)$ with respect to ρ give the n-point functions at *zero external momenta* as a function of κ. We shall be mostly concerned in this paper with the critical regime where $\rho_0(\kappa=0)=0$, and hence in n-point functions in vanishing external field, for which we shall introduce special notation. We set

$$m_\kappa^2 \equiv \left.\frac{dV_\kappa}{d\rho}\right|_{\rho=0}, \quad g_\kappa \equiv \left.\frac{d^2V_\kappa}{d\rho^2}\right|_{\rho=0}, \quad h_\kappa \equiv \left.\frac{d^3V_\kappa}{d\rho^3}\right|_{\rho=0}. \tag{23}$$

For vanishing external field the propagator is diagonal, $G_{12}(\kappa;q) = \delta_{12}G_{LPA'}(\kappa;q)$, with

$$G_{LPA'}^{-1}(\kappa;q) = Z_\kappa q^2 + R_\kappa(q) + m_\kappa^2. \tag{24}$$

For the n-point functions $\Gamma^{(4)}$ and $\Gamma^{(6)}$, we have, respectively,

$$\Gamma_{1234}^{(4)LPA'}(\kappa) = g_\kappa(\delta_{12}\delta_{34} + \delta_{13}\delta_{24} + \delta_{14}\delta_{23}), \tag{25}$$

and

$$\begin{aligned}\Gamma_{123456}^{(6)LPA'}(\kappa) = h_\kappa[&\delta_{56}(\delta_{12}\delta_{34} + \delta_{13}\delta_{24} + \delta_{14}\delta_{23}) + \delta_{46}(\delta_{12}\delta_{35} \\ &+ \delta_{13}\delta_{25} + \delta_{23}\delta_{15}) + \delta_{36}(\delta_{12}\delta_{45} + \delta_{14}\delta_{25} \\ &+ \delta_{15}\delta_{24}) + \delta_{26}(\delta_{13}\delta_{45} + \delta_{14}\delta_{35} + \delta_{15}\delta_{34}) \\ &+ \delta_{16}(\delta_{23}\delta_{45} + \delta_{24}\delta_{35} + \delta_{25}\delta_{34})].\end{aligned} \tag{26}$$

In order to factor out the large variations of the effective potential which arise when κ varies from the microscopic scale Λ to the physical scale $\kappa=0$, and also to exhibit the fixed point structure, it is convenient to isolate the explicit scale factors ($V_\kappa \sim \kappa^d$, $Z_\kappa\rho \sim \kappa^{d-2}$) and to define dimensionless quantities:

$$v_\kappa(z) \equiv K_d^{-1}\kappa^{-d}V_\kappa(\rho), \tag{27}$$

with

$$z \equiv K_d^{-1}Z_\kappa\kappa^{2-d}\rho. \tag{28}$$

In these definitions, for further simplifications, we have also included a factor K_d, which originates from angular integrations:

$$K_d^{-1} \equiv 2^{d-1}\pi^{d/2}d\,\Gamma(d/2). \tag{29}$$

Note that K_d can be a small number, e.g., $K_3 = 1/6\pi^2$. We also introduce dimensionless couplings:

$$m_\kappa^2 \equiv Z_\kappa\kappa^2\hat{m}_\kappa^2, \quad g_\kappa \equiv K_d^{-1}Z_\kappa^2\kappa^{4-d}\hat{g}_\kappa, \quad h_\kappa \equiv K_d^{-2}Z_\kappa^3\kappa^{6-2d}\hat{h}_\kappa, \tag{30}$$

so that

$$\hat{m}_\kappa^2 = \left.\frac{dv_\kappa}{dz}\right|_{z=0}, \quad \hat{g}_\kappa = \left.\frac{d^2v_\kappa}{dz^2}\right|_{z=0}, \quad \hat{h}_\kappa = \left.\frac{d^3v_\kappa}{dz^3}\right|_{z=0}. \tag{31}$$

The solution of the LPA′ is well documented in the literature (see, e.g., Refs. [6,27]). It is convenient to solve the equation for the derivative of the potential with respect to z, i.e., $w_\kappa(z) \equiv \partial_z v_\kappa(z)$, rather than that for the effective potential itself. With the Litim regulator (20), the integrals in Eqs. (17) and (21) can be done analytically. One gets

$$\kappa\partial_\kappa w_\kappa = -(2-\eta_\kappa)w_\kappa + (d-2+\eta_\kappa)zw_\kappa' - \left(1-\frac{\eta_\kappa}{d+2}\right) \times \left(\frac{(N-1)w_\kappa'}{(1+w_\kappa)^2} + \frac{3w_\kappa' + 2zw_\kappa''}{(1+w_\kappa+2zw_\kappa')^2}\right), \tag{32}$$

and

$$\eta_\kappa = \frac{4z_0[w_\kappa'(z_0)]^2}{[1+2z_0w_\kappa'(z_0)]^2}, \tag{33}$$

where $w_\kappa' = \partial_z w_\kappa(z)$, $w_\kappa'' = \partial_z^2 w_\kappa(z)$, and $z_0 = z_0(\kappa)$ is the running minimum of the potential $[w_\kappa(z_0)=0]$. Equations (32) and (33) are solved starting from the initial condition at $\kappa=\Lambda$:

$$w_\kappa(z, \kappa=\Lambda) = \hat{m}_\Lambda^2 + \hat{g}_\Lambda z, \tag{34}$$

where $\hat{m}_\Lambda$ and $\hat{g}_\Lambda$ are related to the parameters r and u of the classical action (1) by

$$\hat{m}_\Lambda^2 = \frac{r}{\Lambda^2}, \quad \hat{g}_\Lambda = \frac{u}{\Lambda^{4-d}}\frac{K_d}{3}. \tag{35}$$

Before looking at some results obtained by solving numerically Eqs. (32) and (33), it is useful to get insight into the expected behavior of the solution by solving Eq. (32) approximately [6], ignoring the anomalous dimension. To this aim, we assume that, for all κ, $w_\kappa(z)$ retains the form of Eq. (34), i.e.,

$$w_\kappa(z) = \hat{m}_\kappa^2 + \hat{g}_\kappa z. \tag{36}$$

The minimum of the potential $z_0(\kappa)$ satisfies $w_\kappa(z_0)=0$, i.e., $z_0(\kappa) = -\hat{m}_\kappa^2/\hat{g}_\kappa$. The equations for $z_0(\kappa)$ and $\hat{g}_\kappa$ are easily obtained from Eq. (32), taking into account that, at criticality, $z_0\hat{g} \ll 1$ to make simplifications whenever appropriate. One gets

$$\kappa\frac{dz_0}{d\kappa} = -(d-2)z_0 + N + 2 - 6z_0\hat{g}_\kappa,$$

$$\kappa\frac{d\hat{g}_\kappa}{d\kappa} = (d-4)\hat{g}_\kappa + 2(N+8)\hat{g}_\kappa^2. \tag{37}$$

The equation for $\hat{g}_\kappa$ defines the usual one-loop β function; in this approximation this equation decouples and can be solved explicitly:

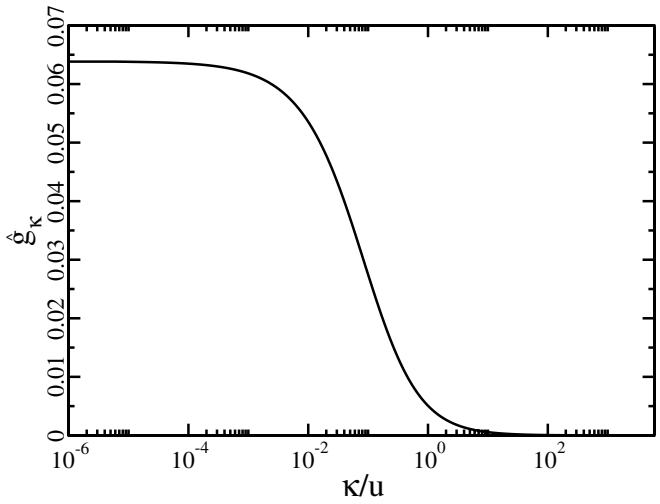

FIG. 5. The dimensionless coupling $\hat{g}_\kappa$ as a function of κ/u (in a logarithmic scale) obtained by solving the LPA′ equations for $N=2$ and $d=3$. The value of $\hat{g}_\kappa$ at the IR fixed point is $\hat{g}^*=0.064$. The value of κ for which $\hat{g}_\kappa = \hat{g}^*/2$ is $\kappa_c = 0.072$.

$$\hat{g}_\kappa = \frac{\hat{g}^*}{1+\left(\frac{\kappa}{\kappa_c}\right)^{4-d}}, \tag{38}$$

where $\hat{g}^*$ is the value of $\hat{g}$ at the infrared (IR) fixed point, $\hat{g}^* = (4-d)/[2(N+8)]$, and κ_c is the value of κ for which $\hat{g}_\kappa = \hat{g}^*/2$. We have ($\hat{g}^* \gg \hat{g}_\Lambda$)

$$\left(\frac{\kappa_c}{\Lambda}\right)^{d-4} = \frac{\hat{g}^* - \hat{g}_\Lambda}{\hat{g}_\Lambda} \approx \frac{\hat{g}^*}{\hat{g}_\Lambda}. \tag{39}$$

$\kappa_c^{4-d} = uK_d/(3\hat{g}^*)$ is the typical scale which separates the scaling region, dominated by the IR fixed point, where $\hat{g}=\hat{g}^*$, from the perturbative region, dominated by the UV fixed point $\hat{g}=0$ (when $\kappa \gg \kappa_c$, one can expand $\hat{g}_\kappa$ in powers of κ_c/κ; in leading order $g_\kappa = (u/3)[1-(\kappa_c/\kappa)^{4-d}]$).

We show in Figs. 5 and 6 the dimensionless coupling $\hat{g}_\kappa$ and the anomalous dimension η_κ obtained by solving the complete LPA′ equations numerically for $d=3$ and $N=2$. The coupling constant $\hat{g}_\Lambda$ has been fixed to a small value, and $\hat{m}_\Lambda^2$ has been adjusted in order to reach the IR fixed point as $\kappa \to 0$. Note that w_κ depends *a priori* on u, κ, and Λ, but since it is dimensionless, it can only depend on the ratios κ/u and u/Λ (in $d=3$). However, because the theory is superrenormalizable in $d=3$, w_κ becomes independent of u/Λ in the limit of large Λ. One finds numerically that this regime is attained when $u/\Lambda \lesssim 10^{-3}$, a condition satisfied in all numerical results presented in this paper: more precisely, we used $u/\Lambda = 3K_3^{-1} \times 10^{-6} \simeq 1.8 \times 10^{-4}$, i.e., $\hat{g}_{\kappa=\Lambda} = 10^{-6}$; the corresponding value of $\hat{m}_\Lambda^2$ needed to reach the fixed point is $\hat{m}_\Lambda^2 = -3.999\,527\cdots \times 10^{-6}$. The general behaviors seen in Figs. 5 and 6 are those expected from the approximate analytic solution discussed above, in particular the fixed point values reached at small κ. On a logarithmic scale, the change of regime between the perturbative regime at large κ and the scaling regime at small κ occurs rather rapidly, at the typical

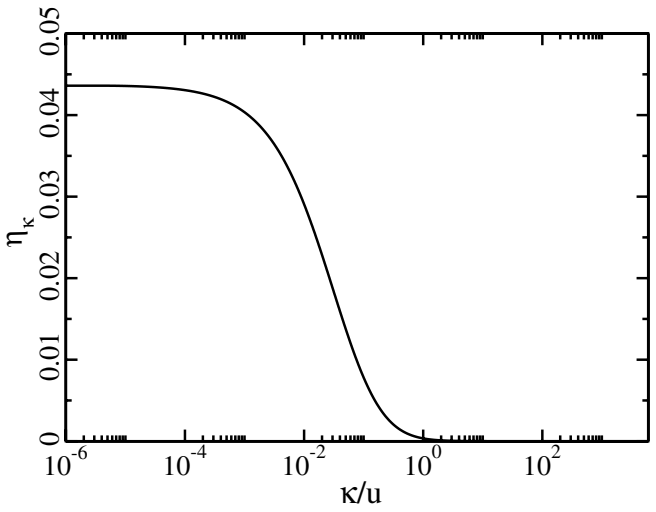

FIG. 6. The anomalous dimension η_κ as a function of κ/u (in a logarithmic scale) obtained by solving the LPA′ equations for $N=2$ and $d=3$. The value of η at the IR fixed point is $\eta^*=0.044$.

scale κ_c. In Fig. 5 $\kappa_c/u \sim 0.07$, not far from the value obtained in the approximate analysis presented above: from Eqs. (35) and (39), for $d=3$ and $N=2$, $\kappa_c/u=20K_3/3 \simeq 0.11$.

Before closing this subsection, let us write the flow equations for the two- and four-point functions in vanishing external field, in the LPA′ limit, in a form that we shall use later. These equations are obtained by differentiating once and twice Eq. (17) with respect to ρ, then setting $\rho=0$, and using the definitions in Eq. (23). They read, respectively

$$\kappa\partial_\kappa m_\kappa^2 = -\frac{(N+2)}{2} g_\kappa I_d^{(2)}, \tag{40}$$

and

$$\kappa\partial_\kappa g_\kappa = (N+8) g_\kappa^2 I_d^{(3)}(\kappa) - \frac{1}{2}(N+4) h_\kappa I_d^{(2)}(\kappa), \tag{41}$$

where we have defined

$$I_d^{(n)}(\kappa) \equiv \int \frac{d^d q}{(2\pi)^d} \kappa\partial_\kappa R_\kappa(q^2) G_{LPA'}^n(\kappa;q)$$
$$= 2K_d \frac{\kappa^{d+2-2n}}{Z_\kappa^{n-1}} \frac{1}{(1+\hat{m}_\kappa^2)^n}\left(1 - \frac{\eta_\kappa}{d+2}\right), \tag{42}$$

the explicit form in the second line being obtained for the Litim regulator. Note that, after going to dimensionless variables and making the same approximations that leads us to Eqs. (37) (neglect the second derivative of w_κ with respect to z, and assume $|\hat{m}_\kappa^2| \ll 1$) one can transform Eq. (41) into the second of Eqs. (37).

For further use, we also rewrite Eq. (41) in the following form:

$$\kappa\partial_\kappa g_\kappa = (N+8) g_\kappa^2 I_d^{(3)}(\kappa)(1 - F_\kappa). \tag{43}$$

where

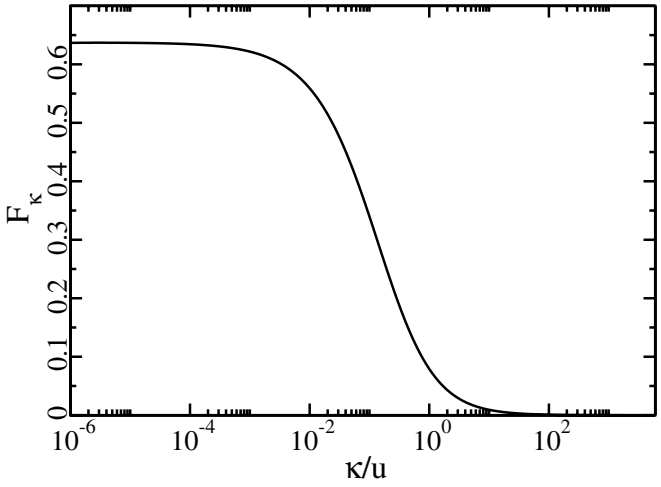

FIG. 7. The function F_κ in Eq. (43) as a function of κ/u (in a logarithmic scale), calculated for $N=2$ and $d=3$.

$$F_\kappa = \frac{1}{2}\frac{N+4}{N+8}\frac{I_d^{(2)}(\kappa)}{I_d^{(3)}(\kappa)}\frac{h_\kappa}{g_\kappa^2} = \frac{1}{2}\frac{N+4}{N+8}(1+\hat{m}_\kappa^2)\frac{\hat{h}_\kappa}{\hat{g}_\kappa^2}. \tag{44}$$

The function F_κ gives a measure of the relative magnitude of the contribution of the six-point vertex term in the flow equation for the four-point function. One can see in Fig. 7 that, as expected, the relative contribution of the six-point vertex is negligible in the perturbative regime ($\kappa \gg \kappa_c$), but becomes of order 1 in the scaling regime ($\kappa \ll \kappa_c$).

D. Correlation functions at large N

In the critical case, the derivative expansion gives accurate results for the correlation functions and their derivatives only at zero external momenta. In order to get insight into the effect of nonvanishing external momenta we consider now the correlation functions in the large N limit (at fixed uN). Our goal here is to illustrate some general features of the momentum dependence of the correlation functions, and how this is affected by the regulator, not to present a consistent discussion of the flow equations and their solutions, which can be found in the literature [11,22,33,34]. Thus we shall not attempt to solve directly the NPRG equations: since they do not close, their solution requires a somewhat elaborate treatment (see, e.g., Ref. [22]). Rather, we shall simply write the solution for the first n-point functions, relying on well known results [35], and verify that they do satisfy the NPRG equations.

For vanishing field, the inverse propagator is of the form

$$G^{-1}(\kappa;q) = q^2 + m_\kappa^2 + R_\kappa(q), \tag{45}$$

where m_κ is a running mass given by a gap equation

$$m_\kappa^2 = r + \frac{Nu}{6}\int \frac{d^d q}{(2\pi)^d}[G(\kappa;q) - G(\Lambda;q)]. \tag{46}$$

The four-point function has the following structure:

$$\Gamma^{(4)}_{1234}(\kappa;p_1,p_2,p_3,p_4) = \delta_{12}\delta_{34}g_\kappa(p_1+p_2) + \delta_{13}\delta_{24}g_\kappa(p_1+p_3) + \delta_{14}\delta_{23}g_\kappa(p_1+p_4), \tag{47}$$

where $g_\kappa(p)$ is given by

$$g_\kappa(p) = \frac{u}{3}\frac{1}{1+\frac{Nu}{6}B_d(\kappa;p)}, \tag{48}$$

with

$$B_d(\kappa;p) \equiv \int \frac{d^dq}{(2\pi)^d} G(\kappa;q)G(\kappa;p+q). \tag{49}$$

Finally we shall need shortly the six-point function $\Gamma^{(6)}_{1234mm}(\kappa;p_1,p_2,p_3,p_4,q,-q)$ (summation over repeated indices is understood)

$$\frac{1}{N}\Gamma^{(6)}_{1234mm}(\kappa;p_1,p_2,p_3,p_4,q,-q) = h_\kappa(p_1+p_2)\delta_{12}\delta_{34} + h_\kappa(p_1+p_3)\delta_{13}\delta_{24} + h_\kappa(p_1+p_4)\delta_{14}\delta_{23}, \tag{50}$$

with

$$h_\kappa(p) = Ng_\kappa(0)g_\kappa^2(p)\int \frac{d^dq}{(2\pi)^d} G^2(\kappa;q)G(\kappa;q+p). \tag{51}$$

All these results can be obtained in a straightforward fashion by calculating the corresponding Feynman diagrams with a regulator. It is, however, easy to verify that the various n-point functions that we have just written are indeed solutions of the flow equations in the large N limit.

To this aim, one notes first that Eq. (9) reduces to an equation for the running mass:

$$\partial_\kappa m_\kappa^2 = -\frac{1}{2}Ng_\kappa(0)\int \frac{d^dq}{(2\pi)^d}\partial_\kappa R_\kappa(q)G^2(\kappa;q), \tag{52}$$

and using Eq. (48), it is easy to check that this equation is equivalent to the gap equation, Eq. (46).

Next, we observe that in the large N limit, a single channel contributes in Eq. (11) for the four-point function; one can then use the following identity in this limit:

$$\Gamma^{(4)}_{12ij}(\kappa;p_1,p_2,q,-q-p_1-p_2)\Gamma^{(4)}_{34ij}(\kappa;p_3,p_4,-q,q-p_3-p_4) = Ng_\kappa^2(p_1+p_2)\delta_{12}\delta_{34}, \tag{53}$$

together with Eq. (50) for $\Gamma^{(6)}$, and obtains

$$\kappa\partial_\kappa g_\kappa(p) = Ng_\kappa^2(p)J_d^{(3)}(\kappa;p) - \frac{N}{2}h_\kappa(p)I_d^{(2)}(\kappa), \tag{54}$$

where the function $I_d^{(2)}(\kappa)$ is that defined in Eq. (42), here with $n=2$ and the propagator (45) replacing $G_{LPA'}$. The function $J_d^{(3)}(\kappa;p)$ is obtained from the general definition

$$J_d^{(n)}(\kappa;p) \equiv \int \frac{d^dq}{(2\pi)^d}\kappa\partial_\kappa R_\kappa(q)G^{n-1}(\kappa;q)G(\kappa;p+q). \tag{55}$$

Note that $J_d^{(n)}(\kappa;p=0) = I_d^{(n)}(\kappa)$. Explicit expressions for the function $J_3^{(3)}(\kappa;p)$ are given in Appendix B.

At this point we remark that the flow equation for $g_\kappa(p)$ can also be obtained directly from the explicit expression (48), in the form

$$\partial_\kappa g_\kappa(p) = -\frac{N}{2}g_\kappa^2(p)\partial_\kappa \int \frac{d^dq}{(2\pi)^d}G(\kappa;q)G(\kappa;q+p). \tag{56}$$

It is then straightforward to verify, using Eqs. (52) and (51) that Eqs. (54) and (56) are indeed equivalent. The first term in Eq. (54) comes from the derivative of the cutoff function in the propagators in Eq. (56), while the second term, which involves the six-point vertex, comes from the derivative of the running mass in the propagators.

Note that Eq. (52) for m_κ and Eq. (54) for $g_\kappa(p=0)$ become identical respectively to Eqs. (40) and (41) of the LPA in the large N limit, a well known property [33].

In view of the approximations that we shall develop in the next section, it is worth analyzing characteristic features of the function $g_\kappa(p)$. For simplicity we specialize for the rest of this subsection to $d=3$. Furthermore, for the purpose of the present, qualitative, discussion, one may assume $m_\kappa=0$. This allows us to obtain easily $g_\kappa(p)$ from Eq. (48) in the two limiting cases $\kappa=0$ and $p=0$. In the first case, we have

$$g_\kappa(0) = \frac{u}{3}\frac{1}{1+\frac{uN}{9\pi^2}\frac{1}{\kappa}}. \tag{57}$$

This is identical to Eq. (38), with here $\hat{g}^* = 1/(2N)$ and $\kappa_c = Nu/9\pi^2$. [The corresponding expressions for Eq. (38) involve $N+8$ instead of N, so that the values of $\hat{g}^*$ and κ_c obtained in the large N limit may be numerically quite different from the actual LPA values when N is not too large, e.g., when $N=2$.] In the other case, we have

$$g_{\kappa=0}(p) = \frac{u}{3}\frac{1}{1+\frac{uN}{48}\frac{1}{p}} = \frac{u}{3}\frac{p}{p+p_c}, \tag{58}$$

with $p_c \equiv uN/48$.

One sees on Eqs. (57) and (58) that the dependence on p of $g_{\kappa=0}(p)$ is quite similar to the dependence on κ of $g_\kappa(p=0)$. In particular both quantities vanish linearly as $\kappa\to 0$ or $p\to 0$, respectively. The result of the complete (numerical) calculation, including the effect of the running mass [i.e., solving the gap equation (46) and calculating $g_\kappa(p)$ from Eq. (48)], can in fact be quite well represented (to within a few percent) for arbitrary p and κ by the following approximate formula:

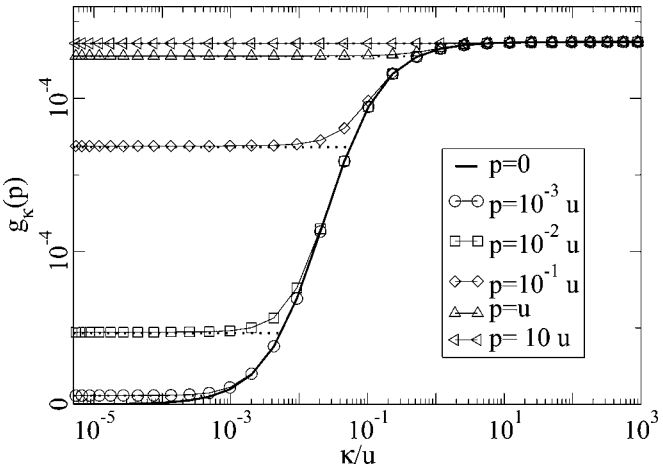

FIG. 8. The function $g_\kappa(p)$ (in units of Λ) obtained from a complete numerical solution of Eqs. (52) and (54), as a function of κ/u (in a logarithmic scale) for five values of p: from bottom to top, $p/u=0.001$, 0.01, 0.1, 1, and 10. The envelope corresponds to $p=0$. This figure illustrates the decoupling of modes: for each value of p, the flow stops when $\kappa \lesssim \alpha p$. The various horizontal asymptotes (dotted lines) correspond to the single value $\alpha=0.54$.

$$g_\kappa(p) \approx \frac{u}{3}\frac{X}{1+X}, \quad X \equiv \frac{\kappa}{\kappa_c}+\frac{p}{p_c}. \tag{59}$$

This simple expression shows that p, when it is nonvanishing, plays the same role as κ as an infrared regulator. In particular, at fixed p, the flow of $g_\kappa(p)$ stops when X becomes independent of κ, i.e., when $\kappa \lesssim p(\kappa_c/p_c)$, with $\kappa_c/p_c=16/3\pi^2\approx 0.54$. This important property of decoupling of the short wavelength modes is illustrated in Fig. 8. As shown by this figure, and also by the expression (59), the momentum dependence of the four-point function can be obtained from its cutoff dependence at zero momentum. In fact Fig. 8 suggests that, to a very good approximation, there exists a parameter α such that $g(\kappa;p)\approx g(\kappa;0)$ when $\kappa > \alpha p$, and $g(\kappa;p)\approx g(\kappa=\alpha p;0)$ when $\kappa < \alpha p$. From the discussion above, one expects $\alpha \approx \kappa_c/p_c=16/3\pi^2\approx 0.54$, which is indeed in agreement with the analysis in Fig. 8.

In order to understand better the origin of this result, we rewrite Eq. (54) as follows:

$$\partial_\kappa g_\kappa(p) = N g_\kappa^2(p) J_d^{(3)}(\kappa;p)[1-F(\kappa,p)], \tag{60}$$

where

$$F(\kappa;p) \equiv \frac{1}{2}\frac{h_\kappa(p) I_d^{(2)}(\kappa)}{g_\kappa^2(p) J_d^{(3)}(\kappa;p)}. \tag{61}$$

When $p=0$, Eq. (60) coincides with the LPA equation (43), and the function $F(\kappa;p)$ with the large N limit of the function F_κ defined for the LPA in Eq. (44). The p dependence of $J_d^{(n)}(\kappa;p)$ is relatively simple: when $p \ll \kappa$, $J_d^{(n)}(\kappa;p) \simeq I_d^{(n)}(\kappa)$; when $p \gg \kappa$, $J_d^{(n)}(\kappa;p)$ vanishes as $1/p^2$. On a logarithmic scale the transition between these two regimes occurs rapidly at momentum $p \sim \kappa$, as illustrated in Fig. 9. Figure 10 shows the similar behavior of the function $h_\kappa(p)/h_\kappa$, where $h_\kappa(p)$is the function (51) which appears in the numerator of

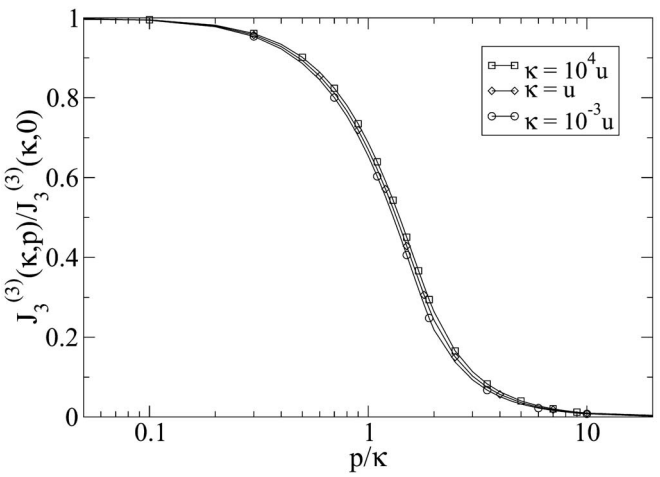

FIG. 9. The function $J_3^{(3)}(\kappa;p)/I_3^{(3)}(\kappa)$ as a function of p/κ (in a logarithmic scale), for different values of κ: $\kappa=10^{-3}u$ (circles), $\kappa=u$ (diamonds), and $\kappa=10^4 u$ (squares).

Eq. (61). Finally, Fig. 11 displays the function $F(\kappa;p)/F_\kappa$: as one can see, the momentum dependence of $F(\kappa;p)$ is nonnegligible only in the region where the function $J_d^{(n)}(\kappa;p)$ is negligible, namely for $\kappa \gtrsim p$. All this suggests that one can rewrite Eq. (60) for $g_\kappa(p)$ as follows:

$$\partial_\kappa g_\kappa(p) \approx N g_\kappa^2(p)\Theta\left(1-\frac{\alpha^2 p^2}{\kappa^2}\right) I_d^{(3)}(\kappa)(1-F_\kappa), \tag{62}$$

where α is a parameter of order unity. Equation (62) is just Eq. (43) in the large N limit, and for $\kappa > \alpha p$. The Θ function ensures that the flow exists only when $\kappa > \alpha p$, and stops for smaller values of κ. These are precisely the features observed in Fig. 8.

III. TOWARDS THE SOLUTION OF THE NPRG EQUATIONS FOR ARBITRARY MOMENTA

Our proposal to solve the NPRG equations for the n-point functions at arbitrary momenta, builds upon the lessons

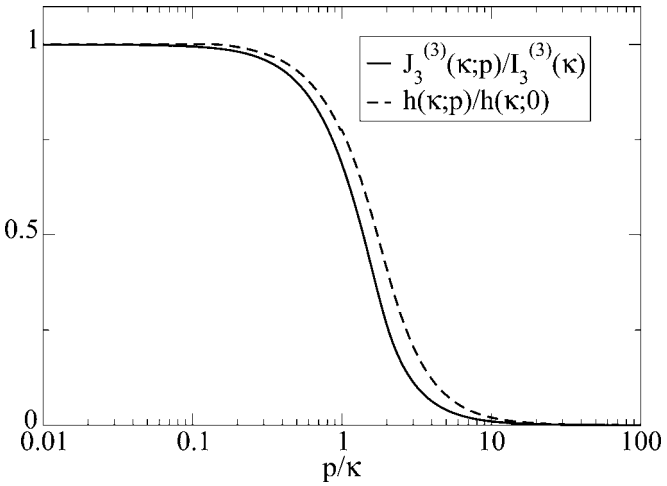

FIG. 10. The function $J_3^{(3)}(\kappa;p)/I_3^{(3)}(\kappa)$ as a function of p/κ (in a logarithmic scale) (full line). The function $h(\kappa;p)/h(\kappa;0)$ as a function of p/κ (dashed line).

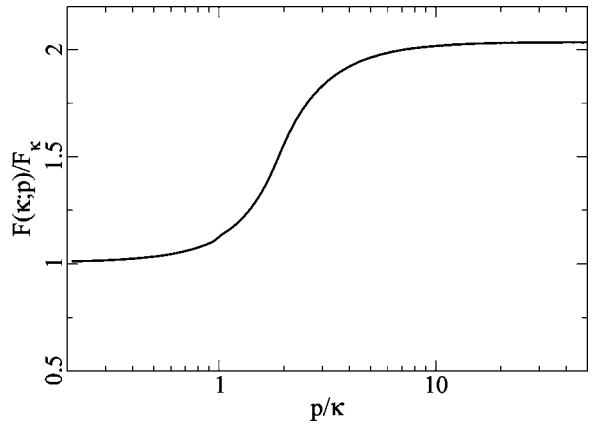

FIG. 11. The function $F(\kappa;p)/F_\kappa$ in the large N-limit [see Eq. (61)] as a function of p/κ (in a logarithmic scale).

learned in the specific examples discussed in the previous section. Namely, we shall take advantage of the decoupling of modes, exploit the solution of the LPA′, and use the possibility to increase accuracy through iterations.

The decoupling of modes is well illustrated in Fig. 8 of the previous section. It suggests that the momentum dependence of the n-point function can be deduced from their κ dependence, as obtained from the LPA′. To be more specific, assume for simplicity that all external momenta are of the same order of magnitude, and call them generically p. Then as long as $\kappa \gtrsim p$, one can use the LPA′ to calculate the n-point functions. When $\kappa \lesssim p$, the flow stops and the n-point functions remain at their values for $\kappa \sim p$. Note that this argument ceases to apply when the momenta enter as exceptional configurations, for which effectively $p=0$. These exceptional configurations cause special difficulties that we shall have to deal with.

The possibility to increase the accuracy through iterations is based on the property recalled in the previous section, that the iteration of the NPRG equations, starting with the classical values of the n-point functions as initial input, reconstructs the usual loop expansion. Thus one may expect to improve the accuracy of the n-point functions at high momenta by iterations. The situation at small momenta is more subtle. Indeed, in the critical regime, iterations may affect the fixed point structure, and may result in unphysical behaviors. This particular feature will be discussed in Paper II.

The procedure that we propose starts with an *initial Ansatz* for the n-point functions to be used in the right-hand side of the flow equations. Integrating the flow equation of a given n-point function gives then the *leading order* (LO) estimate for that n-point function. Inserting the leading order of the n-point functions thus obtained in the right-hand side of the flow equations and integrating gives then the *next-to-leading order* (NLO) estimate of the n-point functions, and so on.

The equations will be solved starting at the bottom of the hierarchy, that is, with the equation for the two-point function. The flow equation for the two-point function involves in its right-hand side the propagator (hence the two-point function), and the four-point function. To determine the two-point function in leading order, we need therefore an initial *Ansatz* for the propagator and the four-point function. Similarly, to get the four-point function in leading order, we need an initial *Ansatz* for the propagator, for the four-point function and the six-point function, and so on.

There is no small parameter controlling the convergence of the process, and the terminology LO, NLO refers merely to the number of iterations involved in the calculation of the n-point function considered. Obviously, the calculations become increasingly complicated as the number of iterations increases, and it is essential that the initial *Ansatz* be as close as possible to the exact solution so that only one or two iterations suffice to get an accurate result. Our main task then is to construct such a good initial *Ansatz*.

A. Construction of the initial *Ansatz*—Generalities

The initial *Ansatz* for the n-point functions are the solutions of approximate flow equations obtained by making the following three approximations.

(*i*) *Vertices are slowly varying functions of the external momenta*. Our first approximation ($\mathcal{A}_1$) exploits a crucial property of the NPRG: the derivative $\partial_\kappa R_\kappa(q)$ limits the range of integrations in the flow equations to $q \lesssim \kappa$. The momentum q enters the vertices in the flow equations typically in the form $\Gamma^{(n)}_{12\cdots n}(\kappa;p_1,p_2,\ldots,p_{n-1}+q,p_n-q)$. Approximation $\mathcal{A}_1$ consists then in assuming that, for any set of external momenta $\{p_1,p_2,\ldots,p_n\}$,

$$\left| \frac{\Gamma^{(n)}_{12\cdots n}(\kappa;p_1,p_2,\ldots,p_{n-1}+q,p_n-q) - \Gamma^{(n)}_{12\cdots n}(\kappa;p_1,p_2,\ldots,p_{n-1},p_n)}{\Gamma^{(n)}_{12\cdots n}(\kappa;p_1,p_2,\ldots,p_{n-1},p_n)} \right| \ll 1. \tag{63}$$

This approximation is justified when the momenta $\{p_1,p_2,\ldots,p_n\}$ are much larger than κ, since then we can neglect q compared to p_i, assuming that $\Gamma^{(n)}$ is a smooth function of the momenta when these are large. In the opposite case of vanishing p_i's, we use the fact that the regulator insures that $\Gamma^{(n)}$ remains a smooth functions of its arguments; in this case, the approximation $\mathcal{A}_1$ is analogous to the leading order in the derivative expansion, i.e., to the LPA, known to be a good approximation.

The approximation $\mathcal{A}_1$ is used to set $q=0$ in the vertices $\Gamma^{(n)}$ and to factor them out of the integrals in the rhs of the flow equations.

(*ii*) *Propagators*. The second approximation ($\mathcal{A}_2$) concerns the propagators in the flow equation, for which we make the replacements

$$G(p+q) \to G_{LPA'}(q)\Theta\left(1-\frac{\alpha^2 p^2}{\kappa^2}\right), \tag{64}$$

where α is an adjustable parameter. A motivation for this approximation is the decoupling of high momentum modes in the flow equations, as illustrated in Sec. II D, and the parameter α will play here a role similar to the one it plays in Sec. II D. A measure of the quality of this approximation is provided by Fig. 9 which shows the ratio $J_3^{(3)}(\kappa;p)/J_3^{(3)}(\kappa;p=0)$ where $J_d^{(n)}(\kappa;p)$ is defined in Eq. (55). $J_3^{(3)}(\kappa;p)$ is the integral which remains in Eq. (11) after approximation $\mathcal{A}_1$ and after choosing as propagator that of the LPA′ (the consistency of this choice will be verified shortly). As seen in Fig. 9, $J_3^{(3)}(\kappa;p)/J_3^{(3)}(\kappa;p=0)$, as a function of p^2/κ^2, looks indeed like a step function, with a weak residual κ dependence.

Different criteria can be used to fix α. One may fix α so that the inflexion point of the curve in Fig. 9 is at $\alpha p=\kappa$. One then obtains, for $N=2$, $\alpha \approx .9$. One can also adjust α so that the integral over κ of $J_3^{(3)}(\kappa;p)$ is identical to that of $J_3^{(3)}(\kappa;0)\Theta(1-\alpha^2p^2/\kappa^2)$. This yields $\alpha \approx 0.6$. We regard these two possible choices as defining roughly the range of "acceptable" values of α, and accordingly we adopt the value $\alpha=0.75\pm0.15$ for our leading order estimate in the case $N=2$. The dependence of the results on the choice of α will be thoroughly discussed in the next section. It represents an important source of theoretical uncertainty on the leading order results which, to a large extent, will be eliminated at next-to-leading order (see Paper II).

Before moving to the next approximation, let us write the equations for the two-point and four-point functions obtained at this stage, i.e., after approximations $\mathcal{A}_1$ and $\mathcal{A}_2$. The equation for the two-point function becomes

$$\kappa\partial_\kappa \Gamma_{12}^{(2)}(\kappa;p) = -\frac{1}{2}\Gamma_{12ll}^{(4)}(\kappa;p,-p,0,0)I_d^{(2)}(\kappa), \tag{65}$$

and that for the four-point function reads

$$\begin{aligned}\kappa\partial_\kappa \Gamma_{1234}^{(4)}(p_1,p_2,p_3,p_4) = I_d^{(3)}(\kappa)\{&\Theta[\kappa^2-\alpha^2(p_1+p_2)^2]\Gamma_{12ij}^{(4)}(p_1,p_2,0,-p_1-p_2)\Gamma_{34ij}^{(4)}(p_3,p_4,0,-p_3-p_4)\\ &+\Theta[\kappa^2-\alpha^2(p_1+p_3)^2]\Gamma_{13ij}^{(4)}(p_1,p_3,0,-p_1-p_3)\Gamma_{24ij}^{(4)}(p_2,p_4,0,-p_2-p_4)+\Theta[\kappa^2-\alpha^2(p_1+p_4)^2]\\ &\times\Gamma_{14ij}^{(4)}(p_1,p_4,0,-p_1-p_4)\Gamma_{32ij}^{(4)}(p_3,p_2,0,-p_3-p_2)\}-\frac{1}{2}\Gamma_{1234ii}^{(6)}(p_1,p_2,p_3,p_4,0,0)I_d^{(2)}(\kappa),\end{aligned} \tag{66}$$

where the function $I_d^{(n)}(\kappa)$ is defined in Eq. (42).

Note that the approximation $\mathcal{A}_2$ amounts to truncate severely the high momentum tails of the propagators. This will cause inaccuracy at high momenta, and a dependence of the leading order results on the value of α.

(*iii*) *Approximation for the* $(n+2)$*-point function*. In order to close the equation for $\Gamma^{(n)}$ we need an approximation for $\Gamma^{(n+2)}$. Namely, we need an approximation for $\Gamma^{(4)}$ in the equation for $\Gamma^{(2)}$ and for $\Gamma^{(6)}$ in the equation for $\Gamma^{(4)}$. Note that we do not want to perform a truncation of the hierarchy, as often done, by setting to zero the higher order n-point functions: indeed in the scaling regime the contributions of all vertices are of the same order of magnitude. Rather, we shall try to obtain a rough estimate for $\Gamma^{(n+2)}$, which is sufficient in order to get the initial *Ansatz* for $\Gamma^{(n)}$ (this rough estimate is not to be confused with the initial *Ansatz* for $\Gamma^{(n+2)}$).

In order to construct this estimate for $\Gamma^{(n+2)}$ we rely on the LPA′ and also use an approximation inspired by the analysis of the correlation functions in the $N\to\infty$ limit of the previous section (Sec. II D). We consider explicitly here the equations for the two-point and the four-point functions.

In the case of the equation for $\Gamma^{(2)}$, one needs an approximation for $\Gamma_{12ll}^{(4)}(\kappa;p,-p,0,0)$, as can be seen in Eq. (65). This can be hinted from Eq. (47), leading us to assume $\Gamma_{12ll}^{(4)}(\kappa;p,-p,0,0)=N\delta_{12}g_\kappa(0)$. The resulting initial *Ansatz* for $\Gamma^{(2)}$ is simply a momentum independent function, the running mass, whose flow equation is given by Eq. (52). Therefore our initial *Ansatz* for the propagator is consistent with Eq. (24), to within the small effect of the anomalous dimension which is ignored at this stage.

We turn now to $\Gamma^{(4)}$. As can be seen in Sec. II D, after doing approximation $\mathcal{A}_2$, the two types of terms in the right-hand side of the flow equation of $\Gamma^{(4)}$ are proportional, with a coefficient that depends only on κ [see Eqs. (54) and (62), and Fig. 11]. Our third approximation ($\mathcal{A}_3$) consists in assuming that this property holds in general, i.e., we set

$$\partial_\kappa \Gamma_{1234}^{(4)[6]}(p_1,p_2,p_3,p_4) = -F_\kappa \partial_\kappa \Gamma_{1234}^{(4)[4]}(p_1,p_2,p_3,p_4), \tag{67}$$

where in the (left-hand side) lhs $\Gamma_{1234}^{(4)[6]}$ is the six-point vertex contribution to the flow of $\Gamma^{(4)}$ [last line in Eq. (66) and Fig. 4], while the term multiplying $-F_\kappa$ in the rhs is that including only four-point vertices [the first three lines in Eq. (66) and Fig. 3]. This relation becomes trivial in the LPA, i.e., when all external momenta are zero. This allows us to fix F_κ from Eq. (44).

Combining all approximations, one gets the following equation that needs to be solved in order to get the initial *Ansatz* for $\Gamma^{(4)}$:

$$\kappa\partial_\kappa\Gamma^{(4)}_{1234}(\kappa;p_1,p_2,p_3,p_4) = I_d^{(3)}(\kappa)(1-F_\kappa)\{\Theta[\kappa^2-\alpha^2(p_1+p_2)^2]\Gamma^{(4)}_{12ij}(p_1,p_2,0,-p_1-p_2)\Gamma^{(4)}_{34ij}(p_3,p_4,0,-p_3-p_4)$$
$$+\Theta[\kappa^2-\alpha^2(p_1+p_3)^2]\Gamma^{(4)}_{13ij}(p_1,p_3,0,-p_1-p_3)\Gamma^{(4)}_{24ij}(p_2,p_4,0,-p_2-p_4)$$
$$+\Theta[\kappa^2-\alpha^2(p_1+p_4)^2]\Gamma^{(4)}_{14ij}(p_1,p_4,0,-p_1-p_4)\Gamma^{(4)}_{32ij}(p_3,p_2,0,-p_3-p_2)\}. \quad (68)$$

In the rest of this section, we construct the solution of this equation in terms of the solution of the LPA′. As a simple illustration of the method to be used, consider first the totally symmetric configuration of momenta: $(p_1+p_2)^2=(p_1+p_3)^2=(p_1+p_4)^2=p^2$ (and $p_1^2=p_2^2=p_3^2=p_4^2=3p^2/4$). One then distinguishes in Eq. (68) two regions, according to the value of κ relative to αp. When $\kappa\geq\alpha p$, all the terms in Eq. (68) are nonzero. One can then verify that the LPA′ expression of $\Gamma^{(4)}$, i.e., that given in Eq. (25), is a solution of the equation. Since the initial condition at $\kappa=\Lambda$ has the form of Eq. (25), and since Eq. (68) is a first order differential equation in κ, the LPA′solution is the unique solution for $\kappa\geq\alpha p$. When $\kappa<\alpha p$, the rhs of Eq. (68) vanishes and the flow stops. In this region, the solution remains the LPA′ solution, but taken at the fixed value $\kappa=\alpha p$. These are the features that we uncovered when we analyzed the correlation functions in the large N limit in Sec. II D.

A similar separation into different regions, according to the value of κ, can be done for general momentum configurations. In all cases, when κ is larger than all the combinations of momenta appearing in the Θ functions in Eq. (68), the solution is simply the LPA′ solution. The other regions, where some of the Θ functions vanish, have to be analyzed case by case. One can then solve Eq. (68) in two steps: first, for one vanishing momentum, $p_3=0$ and $p_4=-p_1-p_2$, then for any combination.

In the next two subsections, in order to simplify the notation, and except when ambiguities may arise, we shall often omit to indicate the explicit κ dependence of $\Gamma^{(4)}$.

B. Calculation of $\Gamma^{(4)}_{1234}(p_1,p_2,0,-p_1-p_2)$

In this case, Eq. (68) reads

$$\kappa\partial_\kappa\Gamma^{(4)}_{1234}(p_1,p_2,0,-p_1-p_2) = I_d^{(3)}(\kappa)(1-F_\kappa)\{\Theta[\kappa^2-\alpha^2(p_1+p_2)^2]\Gamma^{(4)}_{12ij}(p_1,p_2,0,-p_1-p_2)\Gamma^{(4)}_{34ij}(0,-p_1-p_2,0,p_1+p_2)$$
$$+\Theta(\kappa^2-\alpha^2p_1^2)\Gamma^{(4)}_{13ij}(p_1,0,0,-p_1)\Gamma^{(4)}_{24ij}(p_2,-p_1-p_2,0,p_1)$$
$$+\Theta(\kappa^2-\alpha^2p_2^2)\Gamma^{(4)}_{14ij}(p_1,-p_1-p_2,0,p_2)\Gamma^{(4)}_{32ij}(0,p_2,0,-p_2)\}. \quad (69)$$

Notice that in each term in the rhs there is one vertex evaluated with two vanishing momenta. Furthermore, because of the theta functions, each term gives a nonzero contribution only when the remaining nonvanishing momentum is smaller than κ/α. We are therefore in the conditions discussed at the end of the last subsection: the four-point functions with two vanishing momenta are simply the LPA′ ones [Eq. (25)]. By using the fact that Bosonic vertex functions are completely symmetric under simultaneous exchange of internal indices and momenta, we can rewrite Eq. (69) in the following way:

$$\kappa\partial_\kappa\Gamma^{(4)}_{1234}(p_1,p_2,0,-p_1-p_2) = g_\kappa I_d^{(3)}(\kappa)(1-F_\kappa)\times\{\Theta[\kappa^2-\alpha^2(p_1+p_2)^2][\Gamma^{(4)}_{12ii}(p_1,p_2,0,-p_1-p_2)\delta_{34}+\Gamma^{(4)}_{1234}(p_1,p_2,0,-p_1-p_2)$$
$$+\Gamma^{(4)}_{1243}(p_1,p_2,0,-p_1-p_2)]+\Theta(\kappa^2-\alpha^2p_1^2)[\Gamma^{(4)}_{i2i4}(p_1,p_2,0,-p_1-p_2)\delta_{13}+\Gamma^{(4)}_{3214}(p_1,p_2,0,-p_1-p_2)$$
$$+\Gamma^{(4)}_{1234}(p_1,p_2,0,-p_1-p_2)]+\Theta(\kappa^2-\alpha^2p_2^2)[\Gamma^{(4)}_{1ii4}(p_1,p_2,0,-p_1-p_2)\delta_{23}+\Gamma^{(4)}_{1324}(p_1,p_2,0,-p_1-p_2)$$
$$+\Gamma^{(4)}_{1234}(p_1,p_2,0,-p_1-p_2)]\}. \quad (70)$$

This is a first order linear equation where the momenta are parameters. To solve it, we can assume without loss of generality that $p_1^2\geq p_2^2\geq(p_1+p_2)^2$. For the rest of this section, except when that would lead to confusion, we will drop the arguments of $\Gamma^{(4)}_{1234}$, being understood that $\Gamma^{(4)}_{1234}$ refers to $\Gamma^{(4)}_{1234}(\kappa;p_1,p_2,0,-p_1-p_2)$. We need to consider four different regions, according to the value of κ:

(*a*) $\kappa\geq\alpha p_1$. In this region, the solution is identical to that of the LPA′.

(*b*) $\alpha p_1>\kappa\geq\alpha p_2$. In this region, Eq. (70) becomes

$$\kappa\partial_\kappa\Gamma^{(4)}_{1234} = g_\kappa I_d^{(3)}(\kappa)(1-F_\kappa)\{\Gamma^{(4)}_{12ii}\delta_{34}+2\Gamma^{(4)}_{1234}+\Gamma^{(4)}_{1243}$$
$$+\Gamma^{(4)}_{1ii4}\delta_{23}+\Gamma^{(4)}_{1324}\}. \quad (71)$$

To solve this equation, we first notice that the solution is symmetric under the exchange of the second and the fourth internal indices (with no exchange of the momenta), i.e.,

$$\Gamma^{(4)}_{1234}(p_1,p_2,0,-p_1-p_2)=\Gamma^{(4)}_{1432}(p_1,p_2,0,-p_1-p_2). \quad (72)$$

This property is true for $\kappa=\alpha p_1$, and one can verify that it is maintained along the flow. We then look for the general solution symmetric in the indices 2 and 4, in the form

$$\Gamma^{(4)}_{1234}=(\delta_{12}\delta_{34}+\delta_{14}\delta_{32})\Gamma_A+\delta_{13}\delta_{24}\Gamma_B. \quad (73)$$

Substituting Eq. (73) in Eq. (71), one finds the following system of linear equations:

$$\begin{cases} \kappa\partial_\kappa\Gamma_A = I_d^{(3)}(\kappa) g_\kappa (1-F_\kappa)[(N+4)\Gamma_A + 2\Gamma_B] \\ \kappa\partial_\kappa\Gamma_B = I_d^{(3)}(\kappa) g_\kappa (1-F_\kappa)(2\Gamma_A + 2\Gamma_B). \end{cases} \tag{74}$$

The matrix

$$\begin{pmatrix} N+4 & 2 \\ 2 & 2 \end{pmatrix} \tag{75}$$

has the eigenvalues (which are both positives for $N>-2$)

$$\lambda_\pm = \frac{N+6 \pm \sqrt{N^2+4N+20}}{2}, \tag{76}$$

corresponding to the following eigenvectors:

$$\begin{pmatrix} \Gamma_A^\pm \\ \Gamma_B^\pm \end{pmatrix} = \begin{pmatrix} \frac{\lambda_\pm}{2} - 1 \\ 1 \end{pmatrix}. \tag{77}$$

Using these eigenvectors, one can write the general solution of Eq. (74) as

$$\begin{pmatrix} \Gamma_A \\ \Gamma_B \end{pmatrix} = a_\kappa^+ \begin{pmatrix} \Gamma_A^+ \\ \Gamma_B^+ \end{pmatrix} + a_\kappa^- \begin{pmatrix} \Gamma_A^- \\ \Gamma_B^- \end{pmatrix}, \tag{78}$$

where $a_\kappa^\pm$ verify

$$\kappa\partial_\kappa a_\kappa^\pm = I_d^{(3)}(\kappa) g_\kappa (1-F_\kappa)\lambda_\pm a_\kappa^\pm = \frac{\lambda_\pm}{N+8}\kappa\partial_\kappa(\ln g_\kappa) a_\kappa^\pm. \tag{79}$$

We used Eq. (43) to obtain this result. The equation above can be integrated analytically, to give

$$a_\kappa^\pm = a_{\alpha p_1}^\pm \left(\frac{g_\kappa}{g_{\alpha p_1}}\right)^{\lambda_\pm/(N+8)}. \tag{80}$$

By imposing continuity between the two regions (a) and (b) at $\kappa=\alpha p_1$, we obtain then the solution in the region $\alpha p_1 > \kappa \geq \alpha p_2$:

$$\Gamma_{1234}^{(4)} = \frac{g_{\alpha p_1}}{\lambda_- - \lambda_+}\Bigg\{ \delta_{13}\delta_{24}\Bigg[(\lambda_- - 4)\left(\frac{g_\kappa}{g_{\alpha p_1}}\right)^{\lambda_+/(N+8)} - (\lambda_+ - 4) \times \left(\frac{g_\kappa}{g_{\alpha p_1}}\right)^{\lambda_-/(N+8)}\Bigg] + (\delta_{12}\delta_{34} + \delta_{14}\delta_{23}) \times \Bigg[-\lambda_+\left(\frac{g_\kappa}{g_{\alpha p_1}}\right)^{\lambda_+/(N+8)} + \lambda_-\left(\frac{g_\kappa}{g_{\alpha p_1}}\right)^{\lambda_-/(N+8)}\Bigg]\Bigg\}. \tag{81}$$

(c) $\alpha p_2 > \kappa \geq \alpha|p_1+p_2|$. In this region, Eq. (70) becomes

$$\partial_\kappa \Gamma_{1234}^{(4)} = \frac{1}{N+8}\{\Gamma_{12ii}^{(4)}\delta_{34} + \Gamma_{1234}^{(4)} + \Gamma_{1243}^{(4)}\}\partial_\kappa(\ln g_\kappa). \tag{82}$$

We need now the general tensor decomposition:

$$\Gamma_{1234}^{(4)} = \delta_{12}\delta_{34}\Gamma_A + (\delta_{13}\delta_{24} + \delta_{14}\delta_{32})\Gamma_B + (\delta_{13}\delta_{24} - \delta_{14}\delta_{32})\Gamma_C. \tag{83}$$

By substituting in Eq. (82) we get

$$\begin{cases} \partial_\kappa\Gamma_A = \dfrac{1}{N+8}[(N+2)\Gamma_A + 2\Gamma_B]\partial_\kappa(\ln g_\kappa) \\ \partial_\kappa\Gamma_B = \dfrac{2}{N+8}\Gamma_B\partial_\kappa(\ln g_\kappa) \\ \partial_\kappa\Gamma_C = 0. \end{cases} \tag{84}$$

The antisymmetric sector (Γ_C) is decoupled. In order to get the solution in the symmetric sector (Γ_A,Γ_B), we diagonalize the matrix:

$$\begin{pmatrix} N+2 & 2 \\ 0 & 2 \end{pmatrix}, \tag{85}$$

and get the eigenvalues

$$\mu_+ = N+2, \quad \mu_- = 2 \tag{86}$$

corresponding to the eigenvectors

$$\begin{pmatrix} 1 \\ 0 \end{pmatrix}, \quad \begin{pmatrix} 1 \\ -N/2 \end{pmatrix}. \tag{87}$$

One can then write the general solution of the symmetric part of Eq. (84) as

$$\begin{pmatrix} \Gamma_A \\ \Gamma_B \end{pmatrix} = b_\kappa^+ \begin{pmatrix} 1 \\ 0 \end{pmatrix} + b_\kappa^- \begin{pmatrix} 1 \\ -N/2 \end{pmatrix}, \tag{88}$$

where $b_\kappa^\pm$ verifies

$$\kappa\partial_\kappa b_\kappa^\pm = I_d^{(3)}(\kappa) g_\kappa (1-F_\kappa)\mu_\pm b_\kappa^\pm, \tag{89}$$

which, using Eq. (43), leads to

$$b_\kappa^\pm = b_{\alpha p_2}^\pm \left(\frac{g_\kappa}{g_{\alpha p_2}}\right)^{\mu_\pm/(N+8)}. \tag{90}$$

Imposing continuity between the regions (b) and (c), at $\kappa = \alpha p_2$, one obtains finally

$$\Gamma_{1234}^{(4)} = \delta_{12}\delta_{34}\left[b_{\alpha p_2}^+\left(\frac{g_\kappa}{g_{\alpha p_2}}\right)^{\mu_+/(N+8)} + b_{\alpha p_2}^-\left(\frac{g_\kappa}{g_{\alpha p_2}}\right)^{\mu_-/(N+8)}\right] - (\delta_{13}\delta_{24} + \delta_{14}\delta_{32})\frac{N}{2} b_{\alpha p_2}^-\left(\frac{g_\kappa}{g_{\alpha p_2}}\right)^{\mu_-/(N+8)} + (\delta_{13}\delta_{24} - \delta_{14}\delta_{32})\Gamma_{\alpha p_2}^C, \tag{91}$$

where

$$b_{\alpha p_2}^+ = \frac{g_{\alpha p_1}}{\lambda_- - \lambda_+}\left[\left(-\lambda_+ + \frac{1}{N}(\lambda_- - \lambda_+ - 4)\right)\left(\frac{g_{\alpha p_2}}{g_{\alpha p_1}}\right)^{\lambda_+/(N+8)} - \left(-\lambda_- + \frac{1}{N}(\lambda_+ - \lambda_- - 4)\right)\left(\frac{g_{\alpha p_2}}{g_{\alpha p_1}}\right)^{\lambda_-/(N+8)}\right],$$

$$b_{\alpha p_2}^- = -\frac{1}{N}\frac{g_{\alpha p_1}}{\lambda_- - \lambda_+}\left[(\lambda_- - \lambda_+ - 4)\left(\frac{g_{\alpha p_2}}{g_{\alpha p_1}}\right)^{\lambda_+/(N+8)} - (\lambda_+ - \lambda_- - 4)\left(\frac{g_{\alpha p_2}}{g_{\alpha p_1}}\right)^{\lambda_-/(N+8)}\right], \tag{92}$$

$$\Gamma^C_{\alpha p_2} = \frac{g_{\alpha p_1}}{\lambda_- - \lambda_+}\frac{N+2}{2}\left[\left(\frac{g_{\alpha p_2}}{g_{\alpha p_1}}\right)^{\lambda_+/(N+8)} - \left(\frac{g_{\alpha p_2}}{g_{\alpha p_1}}\right)^{\lambda_-/(N+8)}\right]. \tag{93}$$

(*d*) $\alpha|p_1+p_2| > \kappa$. In this region the flow simply stops. The result is then

$$\Gamma^{(4)}_{1234}(\kappa;p_1,p_2,0,-p_1-p_2) = \Gamma^{(4)}_{1234}(\kappa=\alpha|p_1+p_2|;p_1,p_2,0,-p_1-p_2). \tag{94}$$

C. Calculation of $\Gamma^{(4)}_{12ii}(p,-p,q,-q)$

At this point, we could solve Eq. (68) for any combination of momenta, given the fact that once the function is known for the particular combination that has been treated in the last section, all the information appearing in the right-hand side of the equation is known. To give an example we shall consider in this subsection the explicit calculation of $\Gamma^{(4)}_{12ii}(\kappa;p,-p,q,-q)$, when $q \le \kappa$. The result will be used in the next section as the initial *Ansatz* for $\Gamma^{(4)}$ in the calculation of the LO expression of the self-energy. Note that since the favored values of α are smaller than 1, $\alpha q \le \kappa$.

For the considered values of momenta, Eq. (68) becomes

$$\begin{aligned}\kappa\partial_\kappa\Gamma^{(4)}_{12ll}(p,-p,q,-q) &= I^{(3)}_d(\kappa)(1-F_\kappa)\Big[\Gamma^{(4)}_{12ij}(p,-p,0,0)\Gamma^{(4)}_{llij}(q,-q,0,0) \\ &+ \Theta\left(1-\alpha^2\frac{(p+q)^2}{\kappa^2}\right)\Gamma^{(4)}_{1lij}(p,q,0,-p-q) \\ &\times\Gamma^{(4)}_{2lij}(-p,-q,0,p+q) \quad + \Theta\left(1-\alpha^2\frac{(p-q)^2}{\kappa^2}\right) \\ &\times\Gamma^{(4)}_{1lij}(p,-q,0,-p+q)\Gamma^{(4)}_{2lij}(-p,q,0,p-q)\Big].\end{aligned} \tag{95}$$

The rhs of this equation includes the expressions of $\Gamma^{(4)}$ that have been determined in the previous subsection. It is useful to separate the contribution to $\Gamma^{(4)}(\kappa;p,-p,q,-q)$ coming from the first line from those coming from the second and third lines of Eq. (95) above. The first contribution corresponds to the *s* channel, the second corresponds to the sum of the *t* and *u* channels (see Fig. 3).

(*i*) *s channel*. In the *s* channel, there are two kinematical regions:

(*a*) $\alpha p \le \kappa$. In this case, we have

$$\kappa\partial_\kappa\Gamma^{[s]}_{12ll}(p,-p,q,-q) = I^{(3)}_d(\kappa)(1-F_\kappa)g^2_\kappa(N+2)^2\delta_{12}, \tag{96}$$

whose solution is [see, Eq. (43)]

$$\Gamma^{[s]}_{12ll}(p,-p,q,-q) = \frac{(N+2)^2}{N+8}g_\kappa\delta_{12}. \tag{97}$$

(*b*) $\alpha p > \kappa$. In this region, we have

$$\kappa\partial_\kappa\Gamma^{[s]}_{12ll}(p,-p,q,-q) = I^{(3)}_d(\kappa)(1-F_\kappa)(N+2)^2\delta_{12}g_\kappa g_{\alpha p}\left(\frac{g_\kappa}{g_{\alpha p}}\right)^{(N+2)/(N+8)}, \tag{98}$$

whose solution is

$$\Gamma^{[s]}_{12ll}(p,-p,q,-q) = g_{\alpha p}\delta_{12}(N+2)\left\{\frac{N+2}{N+8}+\left(\frac{g_\kappa}{g_{\alpha p}}\right)^{(N+2)/(N+8)}-1\right\}, \tag{99}$$

where we used continuity between the two regions in order to fix the integration constant.

(*ii*) *t and u channels*. Let us now turn to the contribution of the *t* and *u* channels in Eq. (95). Since the two channels only differ in the sign of *q*, we consider only the *t* channel, with kinematical variable $|p+q|$. There are two situations to analyze.

(*A*) $|p+q| > |p|$. In this case, there are two kinematical regions:

(*a*) $\alpha|p+q| \le \kappa$. In this region the contribution in Eq. (68) reads

$$\kappa\partial_\kappa\Gamma^{[t]}_{12ll}(p,-p,q,-q) = I^{(3)}_d(\kappa)(1-F_\kappa)g^2_\kappa 3(N+2)\delta_{12}. \tag{100}$$

The solution is easily obtained by using Eq. (43) in order to eliminate F_κ. One gets

$$\Gamma^{(t)}_{12ll}(p,-p,q,-q) = 3\frac{N+2}{N+8}g_\kappa\delta_{12}. \tag{101}$$

(*b*) $\alpha|p+q| > \kappa$. In this region the flow stops and we obtain

$$\Gamma^{[t]}_{12ll}(p,-p,q,-q) = 3\frac{N+2}{N+8}g_{\alpha|p+q|}\delta_{12}. \tag{102}$$

(*B*) $|p+q| \le p$. In this case there are three kinematical regions:

(*a*) $\alpha p \le \kappa$. This region is identical to (*Aa*) above. The solution is given by Eq. (101). (*b*) $\alpha p > \kappa \ge \alpha|p+q|$. Here the contribution to Eq. (68) becomes

$$\kappa\partial_\kappa\Gamma^{[t]}_{12ll}(p,-p,q,-q) = I_d^{(3)}(\kappa)(1-F_\kappa)\delta_{12}\frac{N+2}{N^2+4N+20}g_{\alpha p}^2\times\left[\left(\frac{3}{2}N^2+6N+30+\frac{N+14}{2}\sqrt{N^2+4N+20}\right)\left(\frac{g_\kappa}{g_{\alpha p}}\right)^{2\lambda_+/(N+8)}\right.$$
$$\left.+\left(\frac{3}{2}N^2+6N+30-\frac{N+14}{2}\sqrt{N^2+4N+20}\right)\left(\frac{g_\kappa}{g_{\alpha p}}\right)^{2\lambda_-/(N+8)}\right] \tag{103}$$

and has as the solution

$$\Gamma^{[t]}_{12ll}(p,-p,q,-q) = 3\delta_{12}\frac{N+2}{N+8}g_{\alpha p}+\delta_{12}\frac{N+2}{N^2+4N+20}g_{\alpha p}$$
$$\times\left\{\frac{(3/2)N^2+6N+30+(N+14)/2\sqrt{N^2+4N+20}}{2\lambda_+-N-8}\left[\left(\frac{g_\kappa}{g_{\alpha p}}\right)^{(2\lambda_+-N-8)/(N+8)}-1\right]\right.$$
$$\left.+\frac{(3/2)N^2+6N+30-(N+14)/2\sqrt{N^2+4N+20}}{2\lambda_--N-8}\left[\left(\frac{g_\kappa}{g_{\alpha p}}\right)^{(2\lambda_--N-8)/(N+8)}-1\right]\right\}, \tag{104}$$

where, again, we have imposed continuity. (*c*) $\kappa<\alpha|p+q|$. In this regime the flow stops. The solution is found by fixing $\kappa=\alpha|p+q|$ in Eq. (104).

IV. LEADING ORDER RESULTS

The self-energy $\Sigma(\kappa;p)$ is obtained by integrating Eq. (9) from the microscopic scale Λ to the given value of the parameter κ:

$$\delta_{12}\Sigma(\kappa;p) = \delta_{12}r-\frac{1}{2}\int_\Lambda^\kappa d\kappa'\int\frac{d^dq}{(2\pi)^d}G^2(\kappa';q)\partial_{\kappa'}R_{\kappa'}(q)$$
$$\times\Gamma^{(4)}_{12ii}(\kappa';p,-p,q,-q), \tag{105}$$

where we have used the boundary condition $\Sigma(\kappa=\Lambda;p)=r$, with r the bare mass. We shall be working in the critical regime, i.e., for a vanishing physical mass. Thus r is supposed to be adjusted so that $\Sigma(\kappa=0;p=0)=0$, that is,

$$\delta_{12}r = -\frac{1}{2}\int_0^\Lambda d\kappa'\int\frac{d^dq}{(2\pi)^d}G^2(\kappa';q)\partial_{\kappa'}R_{\kappa'}(q)$$
$$\times\Gamma^{(4)}_{12ii}(\kappa';0,0,q,-q). \tag{106}$$

One may use this equation to eliminate the explicit r dependence in Eq. (105)

$$\delta_{12}\Sigma(\kappa;p) = -\frac{1}{2}\int_0^\kappa d\kappa'\int\frac{d^dq}{(2\pi)^d}G^2(\kappa';q)\partial_{\kappa'}R_{\kappa'}(q)$$
$$\times\Gamma^{(4)}_{12ii}(\kappa';p,-p,q,-q)$$
$$+\frac{1}{2}\int_0^\Lambda d\kappa'\int\frac{d^dq}{(2\pi)^d}G^2(\kappa';q)\partial_{\kappa'}R_{\kappa'}(q)$$
$$\times[\Gamma^{(4)}_{12ii}(\kappa';p,-p,q,-q)-\Gamma^{(4)}_{12ii}(\kappa';0,0,q,-q)], \tag{107}$$

from which one immediately deduces the following expression for the physical self-energy $\Sigma(p)\equiv\Sigma(\kappa=0;p)$:

$$\delta_{12}\Sigma(p) = \frac{1}{2}\int_0^\Lambda d\kappa'\int\frac{d^dq}{(2\pi)^d}G^2(\kappa';q)\partial_{\kappa'}R_{\kappa'}(q)$$
$$\times[\Gamma^{(4)}_{12ii}(\kappa';p,-p,q,-q)-\Gamma^{(4)}_{12ii}(\kappa';0,0,q,-q)]. \tag{108}$$

This expression automatically satisfies the criticality condition at $\Sigma(p=0)=0$. But, of course, it holds provided Eq. (106) holds.

In the following subsections we study the self-energy at leading order (LO) of our approximation scheme. The leading order consists in using in the rhs of Eq. (107) the initial *Ansatz* for $\Gamma^{(4)}_{12ii}(\kappa';p,-p,q,-q)$ that has been derived in the previous section. Note that for this initial *Ansatz*, $\Gamma^{(4)}_{12ii}(\kappa';0,0,q,-q)$ is given by the LPA′ expression, so that Eq. (106) is satisfied at LO with the value of r obtained by solving the LPA′ [Eq. (106) for r is then equivalent to Eq. (40), a self-consistent equation for the running mass m_κ where the value of r is adjusted so that, for a given value of the bare coupling, $m_\kappa=0$)].

A. Self-energy at LO

As we just mentioned, in order to calculate Σ_{LO}, we use, as input in the rhs of Eq. (107), the initial *Ansatz* for both the propagator and the four-point function. The initial *Ansatz* for the propagator is needed only for $q<\kappa$ and is taken to be the LPA′ propagator [see Eq. (24)]:

$$G^{-1}_{LPA'}(\kappa;q<\kappa) = Z_\kappa q^2+m_\kappa^2+R_\kappa(q) = Z_\kappa\kappa^2(1+\hat{m}_\kappa^2). \tag{109}$$

The initial *Ansatz* for $\Gamma^{(4)}$ was determined in Sec. III C. It depends only on κ, p^2, q^2, and the angle θ between p and q. By performing the integrations over all angles other than θ, one gets

$$\delta_{12}\Sigma_{LO}(\kappa;p) = -\frac{d-1}{4\pi}K_{d-1}\int_0^{\kappa} d\kappa' \frac{1}{Z_{\kappa'}\kappa'^2(1+\hat{m}_{\kappa'}^2)^2}\int_0^{\kappa'} q^{d-1}dq\left[2+\eta_{\kappa'}\left(\frac{q^2}{\kappa'^2}-1\right)\right]\int_0^{\pi} d\theta \sin\theta(1-\cos^2\theta)^{(d-3)/2}$$

$$\times\Gamma^{(4)}_{12ii}(\kappa';p,-p,q,-q) + \frac{d-1}{4\pi}K_{d-1}\int_0^{\Lambda} d\kappa' \frac{1}{Z_{\kappa'}\kappa'^2(1+\hat{m}_{\kappa'}^2)^2}\int_0^{\kappa'} q^{d-1}dq\left[2+\eta_{\kappa'}\left(\frac{q^2}{\kappa'^2}-1\right)\right]\int_0^{\pi} d\theta \sin\theta$$

$$\times(1-\cos^2\theta)^{(d-3)/2}[\Gamma^{(4)}_{12ii}(\kappa';p,-p,q,-q)-\Gamma^{(4)}_{12ii}(\kappa';0,0,q,-q)]. \quad (110)$$

The physical self-energy at LO is then given by

$$\delta_{12}\Sigma_{LO}(p) = \frac{d-1}{4\pi}K_{d-1}\int_0^{\Lambda} d\kappa \frac{1}{Z_{\kappa}\kappa^3(1+\hat{m}_{\kappa}^2)^2}\int_0^{\kappa} q^{d-1}dq\left[2+\eta_{\kappa}\left(\frac{q^2}{\kappa^2}-1\right)\right]\int_0^{\pi} d\theta \sin\theta(1-\cos^2\theta)^{(d-3)/2}$$

$$\times[\Gamma^{(4)}_{12ii}(\kappa;p,-p,q,-q)-\Gamma^{(4)}_{12ii}(\kappa;0,0,q,-q)]. \quad (111)$$

This expression has interesting scaling properties that we shall present for the case $d=3$ (most of the discussion extends to arbitrary dimensions, with the replacement of u by $u^{1/(4-d)}$).

First, a simple analysis shows that $\Sigma_{LO}(p)$ in Eq. (111) can be written in the form $\Sigma_{LO}(p)=u^2\hat{\Sigma}(p/u)$ where $\hat{\Sigma}$ is a dimensionless function. To see that, we note that, as seen in Sec. III C, $\Gamma^{(4)}_{12ii}(\kappa;p,-p,q,-q)$ is proportional to the LPA′ function g_l where $l=\kappa$, αp, or $\alpha|p+q|$. Now, as discussed in Sec. II C, in $d=3$, the dimensionless function $\hat{g}_l \sim l^{d-4}g_l$ only depends on l/u if u/Λ is small enough. It follows that $\Gamma^{(4)}_{12ii}(\kappa;p,-p,q,-q)=u\hat{\Gamma}^{(4)}_{12ii}(\kappa/u;p/u,-p/u,q/u,-q/u)$ where $\hat{\Gamma}^{(4)}_{12ii}$ is a dimensionless function. The result for Σ_{LO} follows after noticing that the remaining dependence in Λ sits in the upper limit of integration: since the integral converges, that dependence becomes negligible when $\Lambda/u \gg 1$.

A similar (but approximate) scaling holds for the dependence on the parameter α. To see that, let us set $q=0$ in the four-point functions in Eq. (111) (similarly to what is done for the approximation $\mathcal{A}_1$ of Sec. III A). Then, by using the explicit expressions of $\Gamma^{(4)}(\kappa;p,-p,0,0)$ presented in Sec. III C, one can verify from Eq. (111) that $\Sigma_{LO}(p)$ is a function of αp only, i.e., $\Sigma_{LO}(p)=\hat{\Sigma}(\alpha p)$. In fact, we expect this property to be best satisfied for low values of α: indeed, since the second line of Eq. (111) is nonvanishing only for $q \le \kappa \le \alpha p$ (see Sec. III C), the smaller the value of α the smaller the domain of variation of q, and the better is the approximation $q=0$. The approximate scaling on α is clearly visible in Fig. 12.

Turning now to the momentum behavior of Σ_{LO}, we note that both the low and high momentum regimes are correctly reproduced, independently of the value of α. At large momenta, we recover the logarithmic behavior predicted by second order perturbation theory, namely $\Sigma(p) \sim \ln(p/u)$. However, the numerical coefficient in front of the logarithm (which does not depend on α) comes about 7% higher than the correct one $[(N+2)u^2/(288\pi^2)]$.

In the low momentum region, we obtain the expected power law behavior $p^2+\Sigma_{LO}(p) \propto p^{2-\eta^*}$. It turns out that the exponent η^* is the value of the function η_κ at the IR fixed point of the LPA′. This is verified numerically with a numerical uncertainty of 0.001, independently of the value of the parameter α. But this is also an exact result at the present level of approximation. To prove this, let us first note that, in Eq. (111), the difference of the two functions $\Gamma^{(4)}$ in the second line is nonvanishing only when $\kappa \sim p$. Indeed, as can be easily seen from their explicit expressions given in Sec. III C, the two functions $\Gamma^{(4)}$ coincide when $\kappa > \alpha p$ and $\kappa > \alpha|p \pm q|$; therefore there are two different situations where the contributions are not zero. The first situation is $\kappa < \alpha p$. This implies that $\kappa < p$ (remember that $\alpha < 1$). The second situation is more subtle. If we have $\kappa < \alpha|p \pm q|$, one has $|p| \ge |p \pm q| - |q| \ge |p \pm q| - \kappa \ge \kappa(1/\alpha - 1)$, where we used the triangular inequality and the fact that $q \le \kappa$. In both situations we found that, as announced, the integrand in Eq. (111) is nonvanishing only when $\kappa < \beta p$, where β is a number of order 1. It follows that if p is in the scaling region, i.e., if $p \ll p_c$ (with $p_c \simeq \kappa_c$), so are all the momentum variables in the integrand of Eq. (111), i.e., p, q, $|p \pm q|$, and κ. Then all the functions appearing in the rhs of Eq. (111) are in the

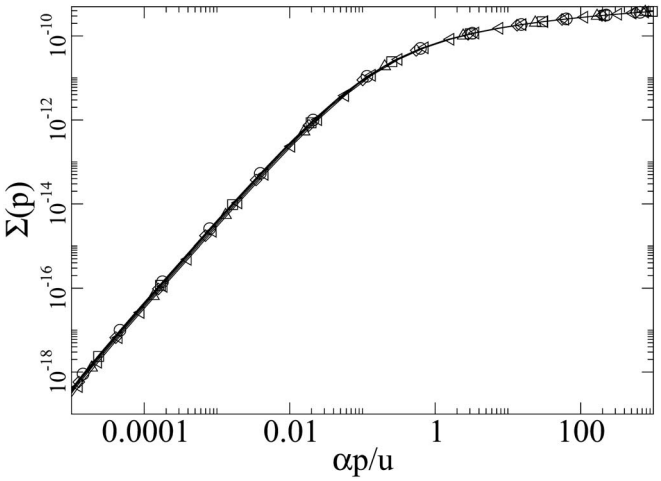

FIG. 12. $\Sigma(p)$ (in units of Λ^2) as a function of $\alpha p/u$ for $N=2$ and various values of α: $\alpha=0.6$ (circles), $\alpha=0.7$ (square), $\alpha=0.75$ (diamond), $\alpha=0.8$ (triangle up), and $\alpha=0.9$ (triangle left). The curves exhibit the α scaling explained in the text.

scaling regime, and their dependence on κ is controlled by the IR fixed point:

$$\hat{m}_\kappa^2 \simeq \hat{m}^{*2}, \quad \hat{g}_\kappa \simeq \hat{g}^*, \quad \eta_\kappa \simeq \eta^*, \quad Z_\kappa \propto \kappa^{-\eta^*}, \quad (112)$$

where we used Eq. (22). Then, from Eq. (30), we get

$$g_\kappa \propto \kappa^{4-d-2\eta^*}. \quad (113)$$

At this point we perform the change of variables $\kappa=px$ and $q=py$ in order to make explicit the p dependence of $\Sigma(p)$ in Eq. (111): we collect a factor p^{η^*} from Z_κ^{-1} and an overall factor p^{d-2} due to the terms $d\kappa$, dq, κ^{-3}, and q^{d-1} appearing in the integrand. As for the p dependence of the four-point functions, one uses the fact that $\Gamma^{(4)}(\kappa;p,-p,q,-q)$ is proportional to $g_l f(g_\kappa/g_l)$ where l is either αp or $\alpha|p\pm q|$, and f is a dimensionless function (see Sec. III C). After the change of variables, using Eq. (113), $\Gamma^{(4)}(\kappa;p,-p,q,-q) - \Gamma^{(4)}(\kappa;p,-p,0,0)$ can thus be written as $p^{4-d-2\eta^*}$ times a function of x and y. Altogether, and using the fact that, as shown above, $\Sigma_{LO}(p)=u^2\tilde{\Sigma}(p/u)$, one gets

$$\Sigma_{LO}(p) = \mathcal{C} u^{\eta^*} p^{2-\eta^*}, \quad (114)$$

where the proportionality coefficient $\mathcal{C}$ is the remaining dimensionless and finite integral over x, y (and θ), which only depends on the parameter α.

The anomalous dimension obtained from the present calculation is then identical to that calculated in the LPA′ [see Eqs. (21) and (22)]. Its value, $\eta^* \sim 0.044$ is to be compared with the best estimates available in the literature, e.g., $\eta = 0.0354 \pm 0.0025$ [36]. A simple proof that the dependence of the field renormalization factor on the scale κ determines in general the momentum dependence of the self-energy (thus defining the anomalous dimension) is presented in Appendix A. However, there is no guarantee that this property should hold in any approximation (for instance, it does not hold in the derivative expansion). It is therefore gratifying to see that the power law behavior expected for the momentum dependence of the self-energy in the scaling regime comes out naturally in the LO of the present approximation scheme.

B. Calculation of $\Delta\langle\varphi^2\rangle$

As a further test of the quality of the leading order result for the self-energy, we have used Σ_{LO} to calculate the shift ΔT_c of the transition temperature of a dilute, weakly interacting, Bose gas. It has been shown that ΔT_c is linear in $an^{1/3}$ [14], where a is the scattering length and n the particle density:

$$\frac{\Delta T_c}{T_c^0} = c a n^{1/3}. \quad (115)$$

Here T_c^0 is the condensation temperature of the ideal gas and $\Delta T_c = T_c - T_c^0$ with T_c the transition temperature of the interacting system. As shown in Ref. [14], the coefficient c can be related to the change $\Delta\langle\varphi^2\rangle$ in the magnitude of the fluctuations of the field described by the action (1),

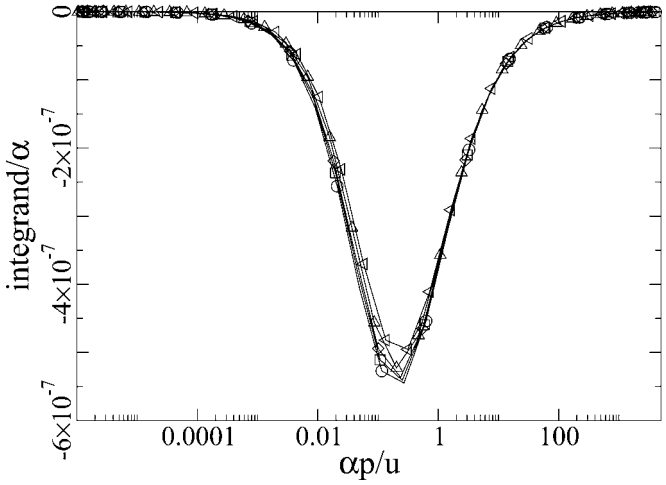

FIG. 13. The integrand of Eq. (117) (divided by α, and in units of Λ) as a function of $\alpha p/u$ for various values of α: $\alpha=0.6$ (circles), $\alpha=0.7$ (square), $\alpha=0.75$ (diamond), $\alpha=0.8$ (triangle up), and $\alpha=0.9$ (triangle left) [points shown are those needed to the numerical calculation of the integral in Eq. (117)], for $N=2$. The curves exhibit the approximate α scaling explained in the text.

$$c = -\frac{256\pi^3}{[\zeta(3/2)]^{4/3}} \frac{\Delta\langle\varphi_i^2\rangle}{Nu}, \quad (116)$$

in the limit $u \to 0$ (and for $N=2$).

The best numerical estimates for $\Delta\langle\varphi^2\rangle$, and hence for c, are those which have been obtained using the lattice technique by two groups, with the results: $c=1.32\pm0.02$ [18] and $c=1.29\pm0.05$ [19]. The availability of these results has turned the calculation of c into a testing ground for other nonperturbative methods: expansion in $1/N$ [17,37], optimized perturbation theory [38,39], resummed perturbative calculations to high loop orders [40]. Note that while the latter methods yield critical exponents with several significant digits, they predict c with only a 10% accuracy. This illustrates the difficulty of getting an accurate determination of c using (semi)analytical techniques.

To understand better the origin of the difficulty, let us write $\Delta\langle\varphi_i^2\rangle$ as the following integral:

$$\frac{\Delta\langle\varphi_i^2\rangle}{N} = \int \frac{d^3p}{(2\pi)^3}\left(\frac{1}{p^2+\Sigma(p)} - \frac{1}{p^2}\right) = -\frac{1}{2\pi^2}\int \frac{dp}{p}\left(p - \frac{p^3}{p^2+\Sigma(p)}\right), \quad (117)$$

where $\Sigma(p)$ is the self-energy at criticality, i.e., $\Sigma(0)=0$. In Eq. (117), the term within the square brakets, to be referred below as the integrand, is, to a very good approximation, equal to $\Sigma(p)/p$ (one finds numerically that this is a good approximation as soon as $p/u \gtrsim 10^{-5}$). As we shall see shortly, $\Sigma(p)/p$ is peaked in the region of intermediate momenta between the critical region and the high momentum perturbative region (see Fig. 13). The difficulty in getting a precise evaluation of the integral (117) is that it requires an accurate determination of $\Sigma(p)$ in a large region of momenta including the crossover region between two different physi-

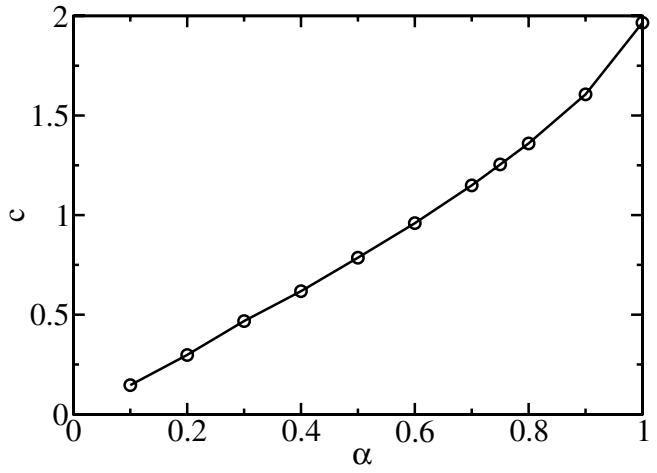

FIG. 14. The coefficient c calculated in LO as a function of the parameter α, for $N=2$.

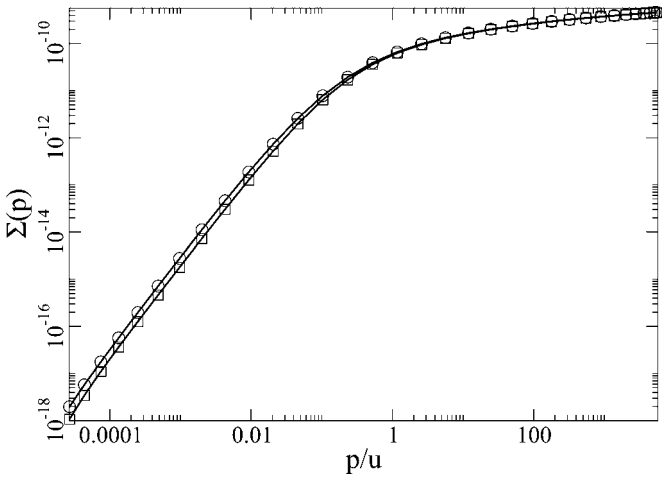

FIG. 15. Calculation of the self-energy (in units of Λ^2, for $N=2$) used to test approximation $\mathcal{A}_1$, as explained in the text: the complete expression of $\Sigma(p)$ (triangles) and the approximate one (squares).

cal regimes [15,17]. In that sense, the calculation of c can be viewed as a very stringent test of the approximation scheme.

A plot of the integrand of Eq. (117) (divided by α) is shown in Fig. 13, for various values of α. As announced, the momentum at which the integrand reaches its maximum lies in the intermediate momentum region: in Fig. 13 this is $\alpha p/u \simeq 0.2$. The approximate scaling behavior that can be observed in Fig. 13 follows from the property of the self-energy discussed in Sec. IV A: as we have seen there, $\Sigma_{LO}(p;\alpha) \simeq \bar{\Sigma}(\alpha p)$, so that, setting $\bar{p}=\alpha p$

$$\frac{\Delta\langle\varphi_i^2\rangle}{N} \approx -\alpha \int \frac{d^3\bar{p}}{(2\pi)^3} \frac{\bar{\Sigma}(\bar{p})}{\bar{p}^4}. \tag{118}$$

Figure 14 shows the value of the coefficient c as a function of α. The (almost) linear behavior of c as a function of α follows directly from Eq. (118). Deviations from the linear behavior can be seen for $\alpha \gtrsim 0.7$: as we have discussed in the previous subsection, for these large values of α, the approximation $\Sigma_{LO}(p;\alpha) \simeq \bar{\Sigma}(\alpha p)$ becomes less accurate. As we can see, when $\alpha=0.75\pm0.15$, one gets $c=1.3\pm0.3$. This result confirms the quality of the leading order expression of the self-energy for all values of the momentum.

We have also calculated Σ_{LO} for different values of N, and compared the corresponding results with those obtained by different means and available in the literature. The quality of our numerical estimates remains of the same level as long as $N \lesssim 50$, but for larger values of N, the calculations lose accuracy. The range of acceptable values of α (see Sec. III A) remains the interval $\sim 0.6-0.9$, and the resulting error bars on the predicted value of c stay of the order of 23–29 %. One gets, for $N=1$, $c=1.06\pm0.27$; for $N=3$, $c=1.47\pm0.39$; for $N=4$, $c=1.66\pm0.44$; for $N=10$, $c=2.33\pm0.60$; for $N=40$, $c=2.97\pm0.63$. These numbers are to be compared with those obtained using other methods; lattice calculation [41] or re-summed perturbation theory carried up to seven-loop order [40] give for $N=1$, $c=1.09\pm0.09$ (lattice) and $c=1.07\pm0.10$ (seven loops); for $N=3$, $c=1.43\pm0.11$ (seven loops); for $N=4$, $c=1.60\pm0.10$ (lattice), and $c=1.54\pm0.11$ (seven loops). The exact result for $N\to\infty$ is also known [17]: $c=2.33$. One observes that, for all values of N, the best accepted results always lie within the error bars of our LO prediction (as obtained from the criteria that were used to fix the range of acceptable values of α in Sec. III A); they approach the lower limit of the band when N grows [the origin of the latter property can in fact be understood by analyzing the steps leading to Eq. (62)].

At this point, we would like to mention another calculation of ΔT_c using the nonperturbative renormalization group [42]. A value $c=1.23$ has been obtained there for $N=2$, which looks in good agreement with the lattice result. However, for reasons that will be detailed in Paper II, the approximation scheme used in Ref. [42] makes it very hard to gauge the quality of this prediction.

Before finishing this section we present a consistency check of the approximation $\mathcal{A}_1$ made in Sec. III A to construct the initial *Ansatz* for the four-point function $\Gamma^{(4)}$. This approximation consists in neglecting the internal momentum dependence in the four-point vertices appearing in the rhs of the flow equation. This was done in order to obtain Eq. (66) for $\Gamma^{(4)}$. Here we shall make this approximation $\mathcal{A}_1$ in the equation for the self-energy, Eq. (111). Figure 15 compares the self-energies obtained form Eq. (111) with and without approximation $\mathcal{A}_1$. One can see that the approximate result differs very little from the exact one. It turns out that both the perturbative regime and the exponent in the scaling regime are almost unchanged, most of the difference being concentrated in the intermediate momentum region. This is verified by calculating the coefficient c with and without the approximation $\mathcal{A}_1$: The value obtained with $\mathcal{A}_1$ is about 10% smaller than that obtained with Σ_{LO}. This illustrates the large sensitivity of the coefficient c to variations of the self-energy in the crossover region.

V. CONCLUSIONS

The calculation of the self-energy of the O(N) model demonstrates that the approximation scheme that we have

presented fulfills its goal, that is, it offers a simple way to calculate the full momentum dependence of the n-point functions. The accuracy achieved in the leading order is already satisfactory, over the full momentum range, as shown by the various tests that we performed.

A crucial ingredient in the calculation is the construction of the initial *Ansatz* for the four-point function. That in itself is an important part of the present paper. This initial *Ansatz* is obtained by solving an approximate flow equation derived using well motivated approximations. The resulting four-point function, albeit approximate, exhibits a realistic momentum dependence, also in the entire momentum range. In particular, the power law behavior expected in the scaling regime is reproduced.

The approximations that we have introduced to construct the initial *Ansatz* for the four-point function involve a parameter α that needs to be adjusted in such a way that approximate expressions match best the exact expressions that they are supposed to represent. This introduces a theoretical uncertainty, which, in the case of the calculation of the shift of the Bose-Einstein transition temperature that we have presented, is of the order of 25%.

In a forthcoming paper [20], we shall present results of a next-to-leading order analysis for the self-energy. To do so we shall need to improve the accuracy of the four-point function, as compared to the initial *Ansatz* presented in this paper. That is, we shall calculate the four-point function at leading order, i.e., construct an initial *Ansatz* for the six-point function. The next-to-leading order calculation of the self-energy will allow us to test fully the approximation scheme, and detect some of its weaknesses. As we shall see, the calculation of c will be greatly improved, in particular the dependence on the parameter α will be eliminated, and results obtained in quite good agreement with lattice data.

ACKNOWLEDGMENTS

The diagrams in this paper were made with JAXODRAW [43]. R.M.-G. and N.W. are grateful for the hospitality of the ECT* in Trento where part of this work was carried out.

APPENDIX A: THE FUNCTION η_κ AND THE ANOMALOUS DIMENSION

It is usually accepted [6] that the κ dependence of the field renormalization factor Z_κ (for values of κ where the couplings have approached the infrared fixed point) determines the anomalous dimension of the field. However, it is not *a priori* obvious that the momentum dependence of correlation functions obtained after some approximation follows automatically the corresponding scaling law: this is not so, for instance, in the derivative expansion. We find it therefore useful to present in this appendix a simple derivation of this property. The arguments in the proof given here help to clarify the conditions under which this property will be satisfied in an approximation. This also completes the derivation presented in Sec. IV A, that the anomalous dimension calculated from the momentum dependence of the four-point function obtained as solution of the approximate equation derived in Sec. III is indeed equal to that deduced from the κ dependence of Z_κ calculated in the LPA′.

Let us consider the two-point function $\Gamma^{(2)}(p,\kappa,u)$ for $p,\kappa \ll \kappa_c \sim u^{1/(4-d)}$ in order to be in the scaling regime. Then, scale invariance implies that

$$\frac{\Gamma^{(2)}(p',\kappa,u)}{\Gamma^{(2)}(p,\kappa,u)} = \tilde{f}\left(\frac{p'}{p},\frac{p}{\kappa}\right), \tag{A1}$$

where $\tilde{f}$ is a dimensionless function of its arguments. It follows that

$$\Gamma^{(2)}(p,\kappa,u) = \Gamma^{(2)}(0,\kappa,u) f\left(\frac{p}{\kappa}\right), \tag{A2}$$

where we have set $f(p/\kappa) \equiv \tilde{f}(0,p/\kappa)$. Note that the dependence on the microscopic parameter u is entirely contained in the factor $\Gamma^{(2)}(0,\kappa,u)$ [$\Gamma^{(2)}(0,\kappa,u)$ is well defined thanks to the IR regulator], and the momentum dependence factors out in the scaling function $f(p/\kappa)$. This function has a Taylor expansion at small p/κ, and $f(0)=1$. At this point we may use scale invariance again, together with dimensional analysis, in order to show that in the regime $\kappa \ll \kappa_c$:

$$\Gamma^{(2)}(0,\kappa,u) \propto \kappa^2 \left(\frac{\kappa}{u^{1/(4-d)}}\right)^{-\eta}, \tag{A3}$$

where η is constant. It then follows that for the function $\Gamma^{(2)}(p,\kappa,u)$ in Eq. (A2) to have a limit when $\kappa \to 0$, we must have, for large values of p/κ,

$$f\left(\frac{p}{\kappa}\right) \propto \left(\frac{p}{\kappa}\right)^{2-\eta} \tag{A4}$$

where η is the same constant as in Eq. (A3). Thus

$$\Gamma^{(2)}(p,\kappa,u) \propto p^2 \times \left(\frac{p}{u^{1/(4-d)}}\right)^{-\eta}. \tag{A5}$$

We can write

$$\Gamma^{(2)}(p,\kappa,u) - \Gamma^{(2)}(0,\kappa,u) = Z_\kappa p^2 + O(p^4) \tag{A6}$$

and from Eq. (A2)

$$\Gamma^{(2)}(p,\kappa,u) - \Gamma^{(2)}(0,\kappa,u) = [f(p/\kappa) - 1]\Gamma^{(2)}(0,\kappa,u). \tag{A7}$$

In the regime $\kappa \to 0$, so that Eq. (A3) is valid, and $p \ll \kappa$ so that $f(p/\kappa) \approx 1 + C\,(p/\kappa)^2$, with C a numerical constant, one can then use Eqs. (A3) and (A7) to deduce the behavior of Z_κ:

$$Z_\kappa = C\left(\frac{\kappa}{u}\right)^{-\eta}. \tag{A8}$$

APPENDIX B: THE FUNCTION $J_3^{(3)}(\kappa;p)$

Using the LPA′ propagator [see Eq. (109)] and the regulator of Eq. (20), making the change of variables $\bar{p}=p/\kappa$, $v=q/\kappa$, and $\cos\theta = p\cdot q/pq$, and performing the integrals over the remaining angular variables, one can write Eq. (55) as

$$J_d^{(3)}(\kappa;p) = \frac{\kappa^{d-4}}{Z_\kappa^2(2\pi)^d}\frac{2\pi^{(d-1)/2}}{\Gamma[(d-1)/2]}\frac{1}{(1+\hat{m}_\kappa^2)^2}\int_0^1 dv v^{d-1}\int_0^\pi d\theta \sin\theta(1-\cos^2\theta)^{(d-3)/2}$$
$$\times \frac{(2-\eta+\eta v^2)}{\Theta(1-v^2-\bar{p}^2+2v\bar{p}\cos\theta)+(v^2+\bar{p}^2-2v\bar{p}\cos\theta)\Theta(v^2+\bar{p}^2-2v\bar{p}\cos\theta-1)+\hat{m}_\kappa^2}. \tag{B1}$$

This expression is valid for arbitrary d, but we shall evaluate it only for $d=3$. In order to take care of the Θ functions it is convenient to separate the calculation in two different regions: $2<\bar{p}$ and $\bar{p}\leq 2$. In each case, one performs the θ integral first, and then the integral over v. One gets

(a) $2<\bar{p}$:

$$J_3^{(3)}(\kappa;p) = \frac{1}{\kappa Z_\kappa^2(2\pi)^2}\frac{1}{(1+\hat{m}_\kappa^2)^2}\left(2+\frac{\eta}{2}\left(-\frac{5}{3}+\bar{p}^2-3\hat{m}_\kappa^2\right)\right.$$
$$+\frac{1}{2\bar{p}}\left\{-1+\frac{\eta}{4}+\left(\bar{p}+\sqrt{-\hat{m}_\kappa^2}\right)^2\left[1-\frac{\eta}{2}+\frac{\eta}{4}\left(\bar{p}+\sqrt{-\hat{m}_\kappa^2}\right)^2\right]\right\}\ln\left(\frac{\bar{p}-1+\sqrt{-\hat{m}_\kappa^2}}{\bar{p}+1+\sqrt{-\hat{m}_\kappa^2}}\right)$$
$$\left.+\frac{1}{2\bar{p}}\left\{-1+\frac{\eta}{4}+\left(\bar{p}-\sqrt{-\hat{m}_\kappa^2}\right)^2\left[1-\frac{\eta}{2}+\frac{\eta}{4}\left(\bar{p}-\sqrt{-\hat{m}_\kappa^2}\right)^2\right]\right\}\ln\left(\frac{\bar{p}-1-\sqrt{-\hat{m}_\kappa^2}}{\bar{p}+1-\sqrt{-\hat{m}_\kappa^2}}\right)\right)$$
$$=\frac{1}{\kappa Z_\kappa^2(2\pi)^2}\frac{1}{(1+\hat{m}_\kappa^2)^2}\left[\frac{4}{\bar{p}^2}\left(\frac{1}{3}-\frac{\eta}{15}\right)+\frac{4}{\bar{p}^4}\left(\frac{1}{15}-\frac{\eta}{105}-\frac{\hat{m}_\kappa^2}{3}+\frac{\eta\hat{m}_\kappa^2}{15}\right)+\mathcal{O}[1/(\bar{p}^6)]\right]. \tag{B2}$$

(b) $\bar{p}\leq 2$:

$$J_3^{(3)}(\kappa;p) = \frac{\kappa^{-1}}{Z_\kappa^2(2\pi)^2(1+\hat{m}_\kappa^2)^2}\left(-1+\frac{\eta}{4}+\frac{\eta\hat{m}_\kappa^2}{4}+\bar{p}\left(\frac{3}{2}-\frac{\eta}{8}-\frac{7\eta\hat{m}_\kappa^2}{8}\right)-\frac{3\eta}{4}\bar{p}^2\right.$$
$$+\frac{25\eta}{48}\bar{p}^3+\frac{1}{1+\hat{m}_\kappa^2}\left[\frac{4}{3}-\frac{4\eta}{15}-\bar{p}+\frac{\eta}{3}\bar{p}^2+\left(\frac{1}{12}-\frac{\eta}{6}\right)\bar{p}^3+\frac{\eta}{120}\bar{p}^5\right]$$
$$+\frac{1}{2\bar{p}}\left\{1-\frac{\eta}{4}-\left(\bar{p}+\sqrt{-\hat{m}_\kappa^2}\right)^2\left[1-\frac{\eta}{2}+\frac{\eta}{4}\left(\bar{p}+\sqrt{-\hat{m}_\kappa^2}\right)^2\right]\right\}\ln\left(\frac{\bar{p}+1+\sqrt{-\hat{m}_\kappa^2}}{1+\sqrt{-\hat{m}_\kappa^2}}\right)$$
$$\left.+\frac{1}{2\bar{p}}\left\{1-\frac{\eta}{4}-\left(\bar{p}-\sqrt{-\hat{m}_\kappa^2}\right)^2\left[1-\frac{\eta}{2}+\frac{\eta}{4}\left(\bar{p}-\sqrt{-\hat{m}_\kappa^2}\right)^2\right]\right\}\ln\left(\frac{\bar{p}+1-\sqrt{-\hat{m}_\kappa^2}}{1-\sqrt{-\hat{m}_\kappa^2}}\right)\right)$$
$$=\frac{\kappa^{-1}}{Z_\kappa^2(2\pi)^2(1+\hat{m}_\kappa^2)^2}\left[\frac{4}{3(1+\hat{m}_\kappa^2)}\left(1-\frac{\eta}{5}\right)-\frac{2}{3(1+\hat{m}_\kappa^2)^2}\bar{p}^2\right.$$
$$\left.+\frac{2+\eta-2\hat{m}_\kappa^2+\eta\hat{m}_\kappa^2}{6(1+\hat{m}_\kappa^2)^3}\bar{p}^3-\frac{2(1+\eta-5\hat{m}_\kappa^2+\eta\hat{m}_\kappa^2)}{15(1+\hat{m}_\kappa^2)^4}\bar{p}^4+\mathcal{O}(\bar{p}^5)\right]. \tag{B3}$$

[1] C. Wetterich, Phys. Lett. B **301**, 90 (1993).
[2] U. Ellwanger, Z. Phys. C **58**, 619 (1993).
[3] N. Tetradis and C. Wetterich, Nucl. Phys. B **422**, 541 (1994).
[4] T. R. Morris, Int. J. Mod. Phys. A **9**, 2411 (1994).
[5] T. R. Morris, Phys. Lett. B **329**, 241 (1994).
[6] J. Berges, N. Tetradis, and C. Wetterich, Phys. Rep. **363**, 223 (2002).
[7] C. Bagnuls and C. Bervillier, Phys. Rep. **348**, 91 (2001).
[8] B. Delamotte, D. Mouhanna, and M. Tissier, Phys. Rev. B **69**, 134413 (2004); L. Canet and B. Delamotte, Condens. Matter Phys. **8**, 163 (2005).
[9] S. Weinberg, Phys. Rev. D **8**, 3497 (1973).
[10] U. Ellwanger, Z. Phys. C **62**, 503 (1994); U. Ellwanger, M. Hirsch, and A. Weber, Eur. Phys. J. C **1**, 563 (1998); J. M. Pawlowski, D. F. Litim, S. Nedelko, and L. von Smekal, Phys. Rev. Lett. **93**, 152002 (2004); J. Kato, e-print hep-th/0401068; C. S. Fischer and H. Gies, J. High Energy Phys. 10048 (2004).
[11] U. Ellwanger and C. Wetterich, Nucl. Phys. B **423**, 137 (1994).
[12] For a review, see R. Alkofer and L. von Smekal, Phys. Rep. **353**, 281 (2001).
[13] T. R. Morris, Phys. Lett. B **334**, 355 (1994).

[14] G. Baym, J.-P. Blaizot, M. Holzmann, F. Laloë, and D. Vautherin, Phys. Rev. Lett. **83**, 1703 (1999).
[15] G. Baym, J.-P. Blaizot, M. Holzmann, F. Laloë, and D. Vautherin, Eur. Phys. J. B **24**, 107 (2001).
[16] J. O. Andersen, Rev. Mod. Phys. **76**, 599 (2004).
[17] G. Baym, J-P. Blaizot, and J. Zinn-Justin, Europhys. Lett. **49**, 150 (2000).
[18] P. Arnold and G. D. Moore, Phys. Rev. Lett. **87**, 120401 (2001); Phys. Rev. E **64**, 066113 (2001).
[19] N. V. Prokof'ev and B. V. Svistunov, Phys. Rev. Lett. **87**, 160601 (2001); **87**, 120402 (2001).
[20] J. P. Blaizot, R. Mendez Galain, and N. Wschebor, following paper, Phys. Rev. E **74**, 051117 (2006).
[21] J. P. Blaizot, R. Mendez Galain, and N. Wschebor, Europhys. Lett. **72**, 705 (2005).
[22] J. P. Blaizot, R. Mendez Galain, and N. Wschebor, Phys. Lett. B **632**, 571 (2006).
[23] J. P. Blaizot, R. Mendez Galain, and N. Wschebor, e-print hep-th/0605252.
[24] D. Litim, Phys. Lett. B **486**, 92 (2000); Phys. Rev. D **64**, 105007 (2001); Nucl. Phys. B **631**, 128 (2002); Int. J. Mod. Phys. A **16**, 2081 (2001).
[25] R. D. Ball, P. E. Haagensen, J. I. Latorre, and E. Moreno, Phys. Lett. B **347**, 80 (1995).
[26] J. Comellas, Nucl. Phys. B **509**, 662 (1998).
[27] L. Canet, B. Delamotte, D. Mouhanna, and J. Vidal, Phys. Rev. D **67**, 065004 (2003).
[28] J. Zinn-Justin, *Quantum Field Theory and Critical Phenomena*, Vol. 113 of The International Series of Monographs in Physics (Oxford Science Publications, Oxford, 2002), p. 1.
[29] J. Polchinski, Nucl. Phys. B **231**, 269 (1984).
[30] M. Bonini, M. D'Attanasio, and G. Marchesini, Nucl. Phys. B **409**, 441 (1993).
[31] L. Canet, B. Delamotte, D. Mouhanna, and J. Vidal, Phys. Rev. B **68**, 064421 (2003).
[32] T. R. Morris and M. D. Turner, Nucl. Phys. B **509**, 637 (1998); A. Ringwald and C. Wetterich, *ibid.* **334**, 506 (1990); C. Bervillier, e-print hep-th/0501087.
[33] M. D'Attanasio and T. R. Morris, Phys. Lett. B **409**, 363 (1997).
[34] N. Tetradis and D. F. Litim, Nucl. Phys. B **464**, 492 (1996).
[35] M. Moshe and J. Zinn-Justin, Phys. Rep. **385**, 69 (2003).
[36] R. Guida and J. Zinn-Justin, J. Phys. A **31**, 8103 (1998).
[37] P. Arnold and B. Tomasik, Phys. Rev. A **62**, 063604 (2000).
[38] F. F. de Souza Cruz, M. B. Pinto, R. O. Ramos, F. F. de Souza Cruz, M. B. Pinto, R. O. Ramos, and P. Sena, Phys. Rev. B **64**, 014515 (2001); Phys. Rev. A **65**, 053613 (2002).
[39] J.-L. Kneur, A. Neveu, and M. B. Pinto, Phys. Rev. A **69**, 053624 (2004).
[40] B. Kastening, Phys. Rev. A **68**, 061601(R) (2003); **69**, 043613 (2004).
[41] X. Sun, Phys. Rev. E **67**, 066702 (2003).
[42] S. Ledowski, N. Hasselmann, and P. Kopietz, Phys. Rev. A **69**, 061601(R) (2004); N. Hasselmann, S. Ledowski, and P. Kopietz, Phys. Rev. A **70**, 063621 (2004).
[43] D. Binosi and L. Theussel, Comput. Phys. Commun. **161**, 76 (2004).
[44] Note that depending on the choice of the regulator, not all fluctuations may be suppressed when $\kappa=\Lambda$. However, for renormalizable theories, and if Λ is large enough, the effects of these remnant fluctuations can be absorbed into a redefinition of the parameters of the classical action.
[45] The smoothness of n-point functions would be spoiled by a sharp cutoff regulator. The Litim regulator used in this paper would also lead to difficulties in high orders; however, it allows for a Taylor expansion of n-point functions at leading orders in q^2/κ^2, which is enough for our purposes.